Influence of Multi-atom Bridging Ligands on the Electronic Structure and Magnetic Properties of Homodinuclear Titanium Molecules

Christine M. Aikens[†] and Mark S. Gordon*

Department of Chemistry, Iowa State University, Ames, Iowa 50011

Received: June 20, 2005

The electronic structure and magnetic properties of homodinuclear titanium(III) molecules with bridging ligands from groups 14, 15, and 16 are examined. Single- and multireference methods with triple-ζ plus polarization basis sets are employed. Dynamic electron correlation effects are included via second-order multireference perturbation theory. Isotropic interaction parameters are calculated, and two of the complexes studied are predicted to be ferromagnetic based on multireference second-order perturbation (MRMP2) theory, using the TZVP(fg) basis set. Zero-field splitting parameters are determined using spin−orbit coupling obtained from complete active space (CAS) self-consistent field (SCF) and multiconfigurational quasi-degenerate perturbation theory (MCQDPT) wave functions. Three Breit−Pauli-based spin coupling methods were employed: full Breit−Pauli (HSO2), the partial two-electron method (P2E), and the semiempirical one-electron method (HSO1).

1. Introduction

The interaction of multiple metal centers in molecular complexes, solid-state compounds, and enzymes has become a rapidly expanding field of study over the past few years.[1−6] In particular, the design of single-molecule ferromagnets and antiferromagnetic superconductors with high critical temperatures are significant challenges in the area of materials science. The relationship between magnetic and electronic properties is also a growing field of study in bioinorganic chemistry.[7]

The magnetization of a material depends on the magnetic field acting on it. The magnetic susceptibility, χ, is a property of the material and relates the magnetization, M, to the strength of the magnetic field, H. For relatively low values of H

$$M = \chi H$$

If the magnetic susceptibility is negative, it is independent of temperature and the material is diamagnetic. If the susceptibility is positive, it varies with temperature. This is the case for paramagnetic, ferromagnetic, antiferromagnetic, and ferrimagnetic materials. In ferromagnetic materials, the susceptibility increases as the temperature decreases. In antiferromagnetic materials, the magnetic susceptibility passes through a maximum at the Néel temperature and goes to zero as the temperature approaches absolute zero.

The magnetic behavior of transition metal complexes in which more than one metal atom has unpaired electrons depends on the strength of the interaction between the metal centers. When strong metal−metal bonds occur in a dimer, the molecule will be diamagnetic. If the metal centers do not interact, the magnetic properties of the dimer are unchanged from those of the monomer. In a weakly interacting complex, the weak coupling of the electrons leads to low-lying excited states of different spin. In dinuclear complexes with one unpaired electron on each metal center, the two local spin states S_A and S_B can interact through the bridging ligands with either singlet or triplet coupling. If singlet coupling is favored, the interaction is antiferromagnetic; if triplet coupling is favored, the interaction is ferromagnetic. If this isotropic interaction is the dominant magnetic effect, the total spin quantum number S is a good quantum number.[8]

The Hamiltonian that describes the coupling between local spin operators $\mathbf{S}_A$ and $\mathbf{S}_B$ was introduced by Heisenberg.[9] It may be written as

$$H = -2J\mathbf{S}_A\cdot\mathbf{S}_B$$

where the isotropic exchange interaction parameter J is defined by

$$2J = E(S{=}0) - E(S{=}1)$$

The isotropic interaction parameter is related to the magnetic susceptibility by

$$\chi = \frac{2Ng^2\beta^2}{kT}\left[3 + \exp\left(\frac{-2J}{kT}\right)\right]^{-1}$$

where N is Avogadro's number, g is the average electronic gyromagnetic ratio, β is the Bohr magneton, k is the Boltzmann constant, and T is the temperature. Moreover, for antiferromagnetic compounds, the isotropic interaction parameter is proportional to the Néel temperature T_{max} according to

$$|2J|/kT_{max} = 1.599$$

where $k = 0.695$ cm^{-1} K^{-1}. This relation may be used to compare calculated isotropic interaction parameters with experimentally observable susceptibility maxima.

The isotropic exchange interaction usually has a greater effect on the magnetic properties than other phenomena such as the spin−orbit coupling and the magnetic dipole−dipole interaction. However, if the singlet−triplet splitting is small or if the triplet state is the ground state, these other interactions may become

* To whom correspondence should be addressed. E-mail: mark@si.fi.ameslab.gov.

[†] Current address: Department of Chemistry, Northwestern University, Evanston, IL 60208.

10.1021/jp058191l CCC: $30.25
Published on Web 12/06/2005

essential for an accurate description of the system. In addition, these effects may be seen in an electron paramagnetic resonance (EPR) spectrum of the triplet state, since they result in a zero-field splitting (ZFS) of the M_s components. The Hamiltonian for these terms may be written

$$H = S\cdot\mathbf{D}\cdot S + \beta S\cdot\mathbf{g}\cdot H$$

where the first term accounts for the dipolar and anisotropic exchange interactions due to the zero-field splitting tensor **D**, and the second term accounts for the Zeeman perturbation with the **g** (gyromagnetic) tensor. The principal (diagonal) values of **D** and **g** are fit to the experimental data. The principal values of **D** are used to calculate the axial and nonaxial (rhombic) zero-field splitting parameters D and E according to[10]

$$D = 3D_z/2$$

$$E = (D_x - D_y)/2$$

The anisotropic exchange tensor $\mathbf{D}_e$ may be found by

$$\mathbf{D}_e = \mathbf{D} - \mathbf{D}_d$$

where $\mathbf{D}_d$ is the dipole−dipole interaction tensor. The dipolar term is often the minor contribution to **D** and can often be reasonably estimated from the point dipole approximation.[8] The axial and rhombic exchange interaction parameters, D_e and E_e, are related to the spin−orbit coupling and may be calculated by

$$D = D_d + D_e$$

$$E = E_d + E_e$$

In 1934, Kramers introduced the idea of superexchange in order to explain how transition metal ions in solids could interact at long distances.[11] He proposed that the neighboring nonmagnetic atoms could play a role in the magnetic interaction mechanism through an exchange spin coupling. In the 1950s, Anderson and Nesbet developed basic qualitative models of exchange interactions in solid-state materials.[12−15] The Anderson model has been successful in predicting the sign of the magnetic interaction but does not quantitatively reproduce its magnitude. Early ab initio calculations on the ionic solid $KNiF_3$ confirmed the ideas of the Anderson model but yielded a magnetic coupling value that was much too small.[16]

In 1952, Bleaney and Bowers discovered that superexchange is not limited to solids but also occurs in binuclear or polynuclear metal complexes such as copper acetate.[17] In the mid-1970s, Hay, Thibeault, and Hoffmann (HTH)[18] and Kahn and Briat[19,20] discussed a semiquantitative equivalent of the Anderson model for molecular complexes and other systems based on extended Hückel calculations. One reason that the Anderson and HTH models produce J values that are too small relative to experimental values is that they neglect dynamic correlation contributions. An important advance toward a quantitative examination of magnetic coupling came in 1981, when de Loth et al. used perturbation theory in order to include the effect of excited configuration state functions that contribute to the energy difference between the lowest energy singlet and triplet states.[21] Since this time, perturbation theory methods built on a multireference zeroth-order wave function have been used to examine the magnetic coupling in a variety of metal complexes and materials.[22−40] Other theoretical methods for calculating the magnetic coupling for biradicals and binuclear complexes have been discussed recently.[41]

Ab initio calculations can provide new insights into the interactions between metal centers and ligands. Homodinuclear complexes with one unpaired electron on each metal center, such as d^1 Ti(III) complexes, are some of the simplest model compounds for investigating spin−spin interactions. Experimentally, dititanium(III) compounds with a linear oxo-bridge,[42−45] organic bridge,[46−57] face-sharing bioctahedral tribridge,[58,59] or dibridge (ring) structure have been characterized. Complexes with a ring structure include hydrido-,[60−62] halo-,[63−74] amido-,[75−78] hydroxy-,[74,79] alkoxy-,[76,80] phosphido-,[81] silyl-,[82] sulfato-,[83] and thio-bridged species.[76] Some of the rings are essentially planar[63,66,77,80,81] while others are buckled.[61,79]

The magnetic properties of linear oxo-bridged compounds have been investigated using CASSCF, MC-CEPA, and ACPF calculations[84,85] and density functional theory calculations.[86] The Ti−Ti bonding interaction, isotropic interaction, and zero-field splitting parameters of D_{2h} $H_2Ti(\mu\text{-}H)_2TiH_2$, a simple model of the flat ring compounds, were studied in detail using multireference methods.[29,30] The effects of halide bridging and terminal ligands on the magnetic properties of homodinuclear titanium(III) compounds were also examined using multireference methods.[34] In the present study, the effects of other bridging ligands such as OH, SH, NH_2, PH_2, NNN, CN, OCN, CNO, SCN, NO, and NO_2 on the magnetic properties will be discussed.

2. Computational Details

Geometry optimizations for triplet states were carried out at the restricted open-shell Hartree−Fock (ROHF) level of theory. The triplet orbitals were used as a starting point for a two-configuration self-consistent field (TCSCF) optimization for the singlet states. The basis set used in the geometry optimizations is denoted TZV(p). It consists of a triple-ζ with polarization (14s11p6d/10s8p3d) basis set for titanium, which is comprised of Wachter's basis set[87] with two additional sets of p functions[88] and an additional set of diffuse d functions.[89] In the notation (A/B), A is the primitive basis set and B is the contracted basis set. For hydrogen, Dunning's (5s1p/3s1p) basis set was employed;[90] for carbon, nitrogen, and oxygen, the Dunning (10s6p/5s3p) basis set was used.[91] The McLean and Chandler (12s9p/6s5p) basis set was utilized for phosphorus and sulfur.[92]

The energy second-derivative (Hessian) matrix was calculated and diagonalized at all stationary points. Unless otherwise stated, all stationary points have zero imaginary frequencies and are minima on their respective potential energy surfaces.

Two larger basis sets denoted TZVP(f) and TZVP(fg) were also used in this study. For both, diffuse s and p functions and two sets of d polarization functions were added to the main group elements. The diffuse sp function and 2d polarization function exponents are the default values in GAMESS.[93,94] The basis set called TZVP(f) adds an f function ($\alpha = 0.40$)[95] to the titanium atom. The basis set referred to as TZVP(fg) adds a set of f ($\alpha = 0.591$) and g ($\alpha = 0.390$) polarization functions, as well as a set of diffuse s ($\alpha = 0.035$), p ($\alpha = 0.239$), and d ($\alpha = 0.0207$) functions, to the TZV(p) titanium basis. These exponents in the TZVP(fg) basis set are optimized for correlated titanium atoms.[96]

The effects of dynamic electron correlation were included by carrying out second-order multireference perturbation theory (MRMP2)[97−100] single-point energy calculations at the TCSCF and ROHF geometries. Single-point energy calculations were

TABLE 1: Mulliken Charges on Ti for the Lowest-Energy Singlet and Triplet States

molecule	bonding mode	singlet	triplet
$Ti_2(OH)_2H_4$	1,1-μ-O	1.10	1.11
$Ti_2(SH)_2H_4$	1,1-μ-S	0.87	0.88
$Ti_2(NH_2)_2H_4$	1,1-μ-N	1.06	1.06
$Ti_2(PH_2)_2H_4$	1,1-μ-P	0.79	0.79
$Ti_2(NNN)_2H_4$	1,1-μ	1.07	1.07
$Ti_2(NNN)_2H_4$	1,3-μ	0.96	0.96
$Ti_2(CN)_2H_4$	1,1-μ-C	1.11	1.12
$Ti_2(CN)_2H_4$	1,1-μ-N	1.09	1.09
$Ti_2(CN)_2H_4$	1,2-μ	1.03	1.03
$Ti_2(OCN)_2H_4$	1,1-μ-O	1.14	1.14
$Ti_2(OCN)_2H_4$	1,1-μ-N	1.07	1.07
$Ti_2(OCN)_2H_4$	1,3-μ	1.10	1.10
$Ti_2(ONC)_2H_4$	1,1-μ-O	1.07	1.07
$Ti_2(ONC)_2H_4$	1,1-μ-C	1.12	1.13
$Ti_2(ONC)_2H_4$	1,3-μ	1.01	1.01
$Ti_2(SCN)_2H_4$	1,1-μ-S	0.87	0.87
$Ti_2(SCN)_2H_4$	1,1-μ-N	1.05	1.05
$Ti_2(SCN)_2H_4$	1,3-μ	0.83	0.83
$Ti_2(NO)_2H_4$	1,1-μ-N[a]	1.16	1.16
$Ti_2(NO)_2H_4$	1,1-μ-N[b]	1.00	1.00
$Ti_2(NO)_2H_4$	1,1-μ-O	1.08	1.08
$Ti_2(NO)_2H_4$	1,2-μ	1.09	1.09
$Ti_2(NO_2)_2H_4$	1,3-μ-ONO	1.31	1.31

[a] b_{2u} and b_{1g} frontier molecular orbitals. [b] a_g and b_{1u} frontier molecular orbitals.

repeated with the TZVP(f) and TZVP(fg) basis sets as a test of basis set convergence.

For excited states, fully optimized reaction space (FORS) multiconfigurational SCF (MCSCF) calculations[101−103] (also called complete active space SCF (CASSCF)[104]) with an active space consisting of 2 electrons in 10 or more orbitals are required. Spin−orbit coupling (SOC) effects are determined using both the complete active space SCF (CASSCF-SOC) and multiconfiguration quasi-degenerate perturbation theory (MCQDPT-SOC)[105] methods. Three different operators are used in the calculations: a semiempirical one-electron spin−orbit coupling operator (HSO1),[106] a partial two-electron/full one-electron operator (P2E),[107] and the full Pauli−Breit operator (HSO2).[107]

The electronic structure code GAMESS[93,94] was used for all calculations. Orbitals were visualized using MacMolPlt,[108] a graphical interface to GAMESS.

3. Results and Discussion

Electronic Structure and Energetics. OH. The hydroxide ligand is isoelectronic with fluoride, so it provides a good first comparison with hydride and halide bridging ligands. Indeed, the complex $Ti_2(\mu\text{-}OH)_2H_4$ follows the electronic structure and energetic trends discussed in previous work on Ti_2H_6 [29] and $Ti_2X_2Y_4$ (X,Y = H, F, Cl, Br).[34] Mulliken populations (Table 1) for the TCSCF and ROHF wave functions with the TZV(p) basis show that the titanium atoms are positively charged. The lowest energy D_{2h} singlet and triplet states are determined to be ^1A_g and $^3B_{1u}$, respectively. The molecular orbitals that create these states are primarily formed from the σ and σ^* combination of the $d_{x^2-z^2}$ orbitals on the two Ti atoms (Figure 1), where the Ti atoms lie along the *z*-axis and the OH ligands lie along the *x*-axis. The two configurations that are responsible for the singlet state may be expressed as $[(\sigma)(\sigma^*)]^2$ or

config. no.	σ	σ^*
1	2	0
2	0	2

TABLE 2: Natural Orbital Occupation Numbers (NOONs) from a Natural Orbital Analysis of the MCSCF(2,2) Wave Function

		HOMO		LUMO	
molecule	bonding mode	NOON	sym	NOON	sym
$Ti_2(OH)_2H_4$	1,1-μ-O	1.08	a_g	0.92	b_{1u}
$Ti_2(SH)_2H_4$	1,1-μ-S	1.04	a_1	0.96	b_2
$Ti_2(NH_2)_2H_4$	1,1-μ-N	1.02	a_u	0.98	a_g
$Ti_2(PH_2)_2H_4$	1,1-μ-P	1.05	a_1	0.95	b_2
$Ti_2(NNN)_2H_4$	1,1-μ	1.15	a_g	0.85	b_{1u}
$Ti_2(NNN)_2H_4$	1,3-μ	1.05	a_g	0.95	b_{1u}
$Ti_2(CN)_2H_4$	1,1-μ-C	1.12	a_g	0.88	b_{1u}
$Ti_2(CN)_2H_4$	1,1-μ-N	1.12	a_g	0.88	b_{1u}
$Ti_2(CN)_2H_4$	1,2-μ	1.06	b_u	0.94	a_g
$Ti_2(OCN)_2H_4$	1,1-μ-O	1.06	a_g	0.94	b_{1u}
$Ti_2(OCN)_2H_4$	1,1-μ-N	1.15	a_g	0.85	b_{1u}
$Ti_2(OCN)_2H_4$	1,3-μ	1.02	a_g	0.98	b_u
$Ti_2(ONC)_2H_4$	1,1-μ-O	1.05	a_g	0.95	b_{1u}
$Ti_2(ONC)_2H_4$	1,1-μ-C	1.13	a_g	0.87	b_{1u}
$Ti_2(ONC)_2H_4$	1,3-μ	1.00	a_g	1.00	b_u
$Ti_2(SCN)_2H_4$	1,1-μ-S	1.03	a_1	0.97	b_2
$Ti_2(SCN)_2H_4$	1,1-μ-N	1.13	a_g	0.87	b_{1u}
$Ti_2(SCN)_2H_4$	1,3-μ	1.02	b_u	0.98	a_g
$Ti_2(NO)_2H_4$	1,1-μ-N[a]	1.13	b_{2u}	0.87	b_{1g}
$Ti_2(NO)_2H_4$	1,1-μ-N[b]	1.05	a_g	0.95	b_{1u}
$Ti_2(NO)_2H_4$	1,1-μ-O	1.05	a_g	0.95	b_{1u}
$Ti_2(NO)_2H_4$	1,2-μ	1.03	b_g	0.97	a_u
$Ti_2(NO_2)_2H_4$	1,3-μ-ONO	1.01	b_{1g}	0.99	b_{2u}

[a] b_{2u} and b_{1g} frontier molecular orbitals. [b] a_g and b_{1u} frontier molecular orbitals.

The singlet state has a high degree of diradical character; a natural orbital analysis of the TCSCF/TZV(p) wave function (Table 2) shows that there are 0.92 electrons in the lowest virtual orbital. This suggests that although the molecule is in principle able to form a direct Ti−Ti bond, the singlet state is essentially a singlet diradical with very little bonding interaction.

The TCSCF/TZV(p) energy difference between the singlet and triplet states is only 0.2 kcal/mol (Table 3). The inclusion of dynamic electron correlation via second-order perturbation theory lowers the singlet state preferentially. The MRMP2/TZV(p) energy difference increases to 0.7 kcal/mol. As the basis set size is increased, the singlet−triplet splitting increases by an additional 0.1 kcal/mol to 0.8 kcal/mol at the MRMP2/TZVP(fg) level of theory and is still very small.

To assess the effects of electron correlation on the geometry of the compounds, a numerical MRMP2/TZV(p) optimization was performed for both the singlet and triplet states. At this level of theory, the Ti−Ti distance for the singlet state is predicted to be 3.11Å. The corresponding distance at the TCSCF/TZV(p) level of theory is 3.17Å. The singlet−triplet splitting at the MRMP2/TZV(p) optimized geometries is predicted to be 0.8 kcal/mol, for an increase of 0.1 kcal/mol from the MRMP2//TCSCF/TZV(p) singlet−triplet splitting of 0.7 kcal/mol. In light of these results, MRMP2 optimizations appear to have a minor effect on these compounds and will not be considered further.

SH. The hydrosulfido ligand is isoelectronic with chloride, so one might think that it would follow a similar electronic structure pattern. Unlike $Ti_2(\mu\text{-}OH)_2H_4$, the analogous $Ti_2(\mu\text{-}SH)_2H_4$ D_{2h} structure is not a local minimum. Imaginary frequencies lead to the C_{2v} and C_{2h} structures. The relative energies for these structures are shown in Table 4. The C_{2v} structure is lower in energy than the C_{2h} structure by 1.1 kcal/mol. Geometrical parameters are presented in Table 5. Although it has a lower symmetry, the general electronic structure of $Ti_2(\mu\text{-}SH)_2H_4$ can be related to that of $Ti_2(\mu\text{-}OH)_2H_4$. The frontier molecular orbitals that create the $^1A_1$ and $^3B_2$ states are derived

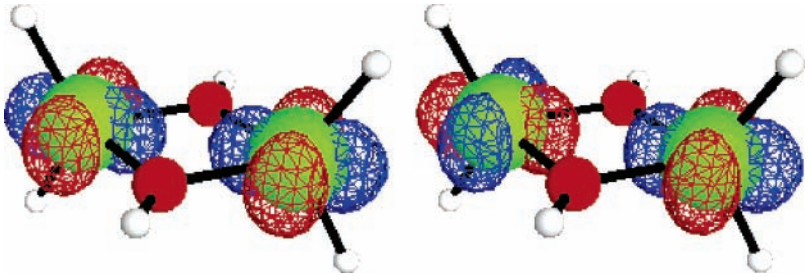

Figure 1. Three-dimensional plots of the σ and σ^* natural orbitals from a two-electron, two-orbital MCSCF/TZV(p) calculation for singlet $Ti_2(OH)_2H_4$. The orbital contour value for the plots is 0.06 $bohr^{3/2}$.

TABLE 3: Calculated Singlet−Triplet Energy Gap (*E*(triplet) − *E*(singlet)) in kcal/mol

molecule	bonding mode	MCSCF/ TZV(p)	MCSCF/ TZVP(f)	MCSCF/ TZVP(fg)	MRMP2/ TZV(p)	MRMP2/ TZVP(f)	MRMP2/ TZVP(fg)
$Ti_2(OH)_2H_4$	1,1-μ-O	0.2	0.2	0.2	0.7	0.8	0.8
$Ti_2(SH)_2H_4$	1,1-μ-S	0.01	0.3	0.3	0.2	0.5	0.5
$Ti_2(NH_2)_2H_4$	1,1-μ-N	0.03	0.03	0.03	0.05	0.07	0.07
$Ti_2(PH_2)_2H_4$	1,1-μ-P	0.01	0.04	0.03	0.2	0.4	0.4
$Ti_2(NNN)_2H_4$	1,1-μ	1.0	1.0	0.9	3.0	3.2	3.2
$Ti_2(NNN)_2H_4$	1,3-μ	0.2	0.07	0.08	0.6	0.5	0.5
$Ti_2(CN)_2H_4$	1,1-μ-C	0.8	0.8	0.8	2.2	2.4	2.5
$Ti_2(CN)_2H_4$	1,1-μ-N	0.8	0.6	0.6	1.9	2.1	2.1
$Ti_2(CN)_2H_4$	1,2-μ	0.2	0.1	0.1	0.7	0.6	0.6
$Ti_2(OCN)_2H_4$	1,1-μ-O	0.2	0.1	0.1	0.5	0.5	0.5
$Ti_2(OCN)_2H_4$	1,1-μ-N	1.1	0.9	0.9	3.0	3.1	3.1
$Ti_2(OCN)_2H_4$	1,3-μ	0.03	0.00	0.01	0.09	0.06	0.06
$Ti_2(ONC)_2H_4$	1,1-μ-O	0.08	0.08	0.08	0.3	0.4	0.4
$Ti_2(ONC)_2H_4$	1,1-μ-C	0.9	1.0	1.0	3.0	3.3	3.3
$Ti_2(ONC)_2H_4$	1,3-μ	−0.01	−0.01	−0.01	−0.03	−0.03	−0.03
$Ti_2(SCN)_2H_4$	1,1-μ-S	−0.02	0.02	0.02	0.03	0.1	0.1
$Ti_2(SCN)_2H_4$	1,1-μ-N	0.9	0.8	0.7	2.6	2.8	2.8
$Ti_2(SCN)_2H_4$	1,3-μ	0.01	0.02	0.02	0.02	0.06	0.06
$Ti_2(NO)_2H_4$	1,1-μ-N[a]	0.9	1.6	1.6	3.2	4.8	4.7
$Ti_2(NO)_2H_4$	1,1-μ-N[b]	0.06	0.06	0.06	0.3	0.3	0.3
$Ti_2(NO)_2H_4$	1,1-μ-O	0.06	0.04	0.04	0.2	0.2	0.2
$Ti_2(NO)_2H_4$	1,2-μ	−0.05	−0.1	−0.1	−0.1	−0.2	−0.2
$Ti_2(NO_2)_2H_4$	1,3-μ-ONO	−0.02	−0.03	−0.03	0.02	0.04	0.03

[a] b_{2u} and b_{1g} frontier molecular orbitals. [b] a_g and b_{1u} frontier molecular orbitals.

TABLE 4: Relative MRMP2/TZV(p) Energies (kcal/mol) for Ligands without Local Minimum D_{2h} σ,σ^* Structure

ligand/structure	state		ligand/structure	state	
μ-SH	singlet	triplet	μ-PH_2	singlet	triplet
D_{2h}	2.3	2.3	D_{2h}	1.0	1.2
C_{2h}	1.1	1.1	C_{2v}	0.0	0.2
C_{2v}	0.0	0.2			
			1,1-μ-SCN	singlet	triplet
μ-NH_2	singlet	triplet	D_{2h}	2.2	2.2
D_{2h} σ,σ^*	5.7	7.8	C_{2h}	0.8	0.7
D_{2h} δ,δ^*	0.3	0.4	C_{2v}	0.0	0.03
C_{2h}	0.0	0.05			

from the Ti $d_{x^2-z^2}$ atomic orbitals. The "modified" σ and σ^* molecular orbitals have a_1 and b_2 symmetries, respectively. The singlet state is essentially a singlet diradical with 0.96 electrons in the lowest virtual orbital (Table 2).

At the TCSCF/TZV(p) level of theory, the singlet state is predicted to be only 0.01 kcal/mol lower in energy than the triplet state (Table 3). The inclusion of dynamic electron correlation at the MRMP2/TZV(p) level further stabilizes the singlet state by 0.2 kcal/mol. As the basis set is improved, the singlet−triplet splitting grows to 0.5 kcal/mol at the MRMP2/TZVP(fg) level of theory.

NH_2. For D_{2h} $Ti_2(\mu\text{-}NH_2)_2H_4$, the $[(\sigma)(\sigma^*)]^2$ orbital configuration is not the dominant configuration in the ground state. Instead, the $[(\delta)(\delta^*)]^2$ orbital configuration (Figure 2) created from the Ti d_{xy} atomic orbitals dominates the ground state, and the $[(\sigma)(\sigma^*)]^2$ orbital configuration corresponds to an excited state. This behavior was noted earlier for $Ti_2(\mu\text{-}F)_2H_4$.[34] MCSCF(2,10) calculations show that the $[(\sigma)(\sigma^*)]^2$ and $[(\delta)(\delta^*)]^2$ configurations essentially do not mix, even though they belong to the same irreducible representation. However, the singlet state comprised of σ orbitals and the triplet state dominated by δ orbitals are not local minima. Imaginary frequencies lead to a C_{2h} structure for both the singlet and triplet states (Figure 3). At the MRMP2/TZV(p) level of theory, this structure is 0.3 and 5.7 kcal/mol lower in energy than the singlet D_{2h} states with orbital configurations $[(\delta)(\delta^*)]^2$ and $[(\sigma)(\sigma^*)]^2$, respectively (Table 4).

PH_2. The lowest energy singlet and triplet states for $Ti_2(\mu\text{-}PH_2)_2H_4$ with D_{2h} symmetry are ^1A_g and $^3B_{1u}$. The D_{2h} triplet state is not a minimum on the potential energy surface. The imaginary frequency ($38i$ cm^{-1}) leads to a structure with C_{2v} symmetry. The lowest energy C_{2v} singlet is 1.0 kcal/mol lower in energy than the lowest energy D_{2h} singlet (Table 4). The ground state of this molecule is more similar to SH than NH_2. The molecular orbitals are formed primarily from the Ti $d_{x^2-z^2}$ orbitals, similar to OH and SH, rather than the d_{xy} orbitals seen in NH_2.

NNN. The azido ligand can act as a bridge between the titanium atoms in two ways: a μ-1,1 ("end-on") mode or a μ-1,3 ("linear") mode. These bridging modes are shown in Figure 4. Both of these bridging modes have been seen experimentally in copper(II) dinuclear compounds.[8] For both modes, the D_{2h} structure is a local minimum. The ground state of these

TABLE 5: Geometrical Parameters for the Lowest Energy Structure of $Ti_2(\mu\text{-}L)_2H_4$

		distances (Å)				bond angles (deg)		dihedral angles (deg)	
$Ti_2(1,1\text{-}\mu\text{-}L)_2H_4$	symmetry	Ti−H	Ti−H	Ti−L	Ti−Ti	L−Ti−L	Ti−L−Ti	H−Ti−Ti−L	Ti−L−Ti−L
$Ti_2(1,1\text{-}\mu\text{-}CN)_2H_4$	D_{2h}	1.743		2.341	3.337	89.1	90.9		
$Ti_2(1,1\text{-}\mu\text{-}CNO)_2H_4$	D_{2h}	1.746		2.326	3.356	87.7	92.3		
$Ti_2(1,1\text{-}\mu\text{-}NCO)_2H_4$	D_{2h}	1.765		2.142	3.193	83.6	96.4		
$Ti_2(1,1\text{-}\mu\text{-}NC)_2H_4$	D_{2h}	1.754		2.185	3.265	83.3	96.7		
$Ti_2(1,1\text{-}\mu\text{-}NCS)_2H_4$	D_{2h}	1.758		2.167	3.242	83.1	96.9		
$Ti_2(1,1\text{-}\mu\text{-}NO)_2H_4$[a]	D_{2h}	1.696		1.928	2.935	80.9	99.1		
$Ti_2(1,1\text{-}\mu\text{-}NNN)_2H_4$	D_{2h}	1.777		2.112	3.226	80.4	99.6		
$Ti_2(1,1\text{-}\mu\text{-}OH)_2H_4$	D_{2h}	1.779		2.037	3.175	77.6	102.4		
$Ti_2(1,1\text{-}\mu\text{-}OCN)_2H_4$	D_{2h}	1.753		2.089	3.296	75.8	104.2		
$Ti_2(1,1\text{-}\mu\text{-}NO)_2H_4$[b]	D_{2h}	1.766		2.214	3.552	73.3	106.7		
$Ti_2(1,1\text{-}\mu\text{-}ON)_2H_4$	D_{2h}	1.762		2.083	3.353	72.9	107.1		
$Ti_2(1,1\text{-}\mu\text{-}ONC)_2H_4$	D_{2h}	1.756		2.081	3.363	72.2	107.8		
$Ti_2(1,1\text{-}\mu\text{-}NH_2)_2H_4$	C_{2h}	1.780		2.151	3.218	83.2	96.8	83.6	
$Ti_2(1,1\text{-}\mu\text{-}SH)_2H_4$	C_{2v}	1.753	1.755	2.575	3.837	79.6	96.3		−21.5
$Ti_2(1,1\text{-}\mu\text{-}PH_2)_2H_4$	C_{2v}	1.765	1.767	2.702	3.927	83.3	93.6		−18.9
$Ti_2(1,1\text{-}\mu\text{-}SCN)_2H_4$	C_{2v}	1.738	1.740	2.628	3.991	74.9	98.8		−26.7

		distances (Å)				bond angles (deg)
$Ti_2(1,2\text{-}\mu\text{-}XZ)_2H_4$ or $Ti_2(1,3\text{-}\mu\text{-}XYZ)_2H_4$	symmetry	Ti−H	Ti−X	Ti−Z	Ti−Ti	X−Ti−Z
$Ti_2(1,2\text{-}\mu\text{-}CN)_2H_4$	C_{2h}	1.756	2.334	2.157	4.573	80.9
$Ti_2(1,3\text{-}\mu\text{-}NNN)_2H_4$	C_{2h}	1.759	2.153	2.153	5.400	88.4
$Ti_2(1,3\text{-}\mu\text{-}OCN)_2H_4$	C_{2h}	1.762	2.079	2.130	5.419	87.0
$Ti_2(1,3\text{-}\mu\text{-}ONC)_2H_4$[c]	C_{2h}	1.760	2.038	2.315	5.562	88.2
$Ti_2(1,3\text{-}\mu\text{-}SCN)_2H_4$	C_{2h}	1.754	2.641	2.117	5.743	94.1
$Ti_2(1,2\text{-}\mu\text{-}NO)_2H_4$[c]	C_{2h}	1.688	1.985	1.783	3.834	96.8
$Ti_2(1,3\text{-}\mu\text{-}ONO)_2H_4$	D_{2h}	1.675	1.797	1.797	4.234	110.6

[a] b_{2u} and b_{1g} frontier molecular orbitals. [b] a_g and b_{1u} frontier molecular orbitals. [c] Triplet state.

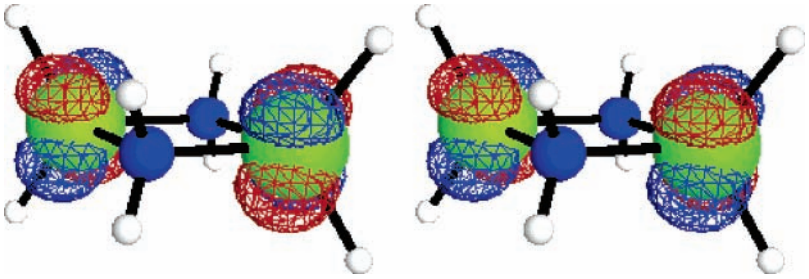

Figure 2. Three-dimensional plots of the δ and δ^* natural orbitals for singlet $Ti_2(NH_2)_2H_4$ from a two-electron, two-orbital MCSCF/TZV(p) calculation. The orbital contour value for the plots is 0.06 $bohr^{3/2}$.

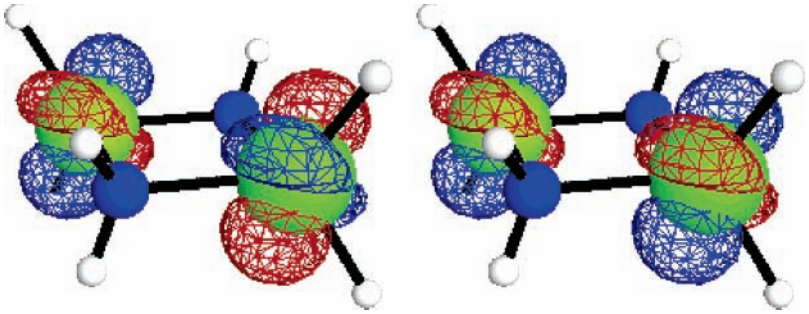

Figure 3. Three-dimensional plots of the natural orbitals for singlet $Ti_2(NH_2)_2H_4$ with C_{2h} symmetry from a two-electron, two-orbital MCSCF/TZV(p) calculation. The orbital contour value for the plots is 0.06 $bohr^{3/2}$.

molecules is ^1A_g, and the lowest energy triplet state is $^3B_{1u}$. The molecular orbitals follow the pattern established for hydroxide. There are 0.85 electrons in the lowest virtual orbital of the end-on structure and 0.95 electrons in the lowest virtual orbital of the linear structure (Table 2) according to a natural orbital analysis of the TCSCF/TZV(p) wave function. The TCSCF/TZV(p) singlet−triplet splitting for the end-on structure is calculated to be 1.1 kcal/mol and increases to 3.2 kcal/mol at the MRMP2/TZVP(fg) level (Table 3). For the linear structure, the TCSCF/TZV(p) singlet−triplet splitting is 0.2 and 0.5 kcal/mol at the MRMP2/TZVP(fg) level. The MRMP2/TZVP(fg) end-on structure is more stable than the linear structure by 1.7 kcal/mol.

Experimentally for the copper compounds, the end-on azido-bridged structures are ferromagnetic, while the linear structures are strongly antiferromagnetic.[109,110] In contrast, the end-on $Ti_2(\mu\text{-}1,1\text{-}NNN)_2H_4$ is very antiferromagnetic and the linear $Ti_2(\mu\text{-}1,3\text{-}NNN)_2H_4$ is slightly antiferromagnetic. The atomic orbitals available to form metal−metal bonds are different on copper and titanium. For copper, the unpaired electron density

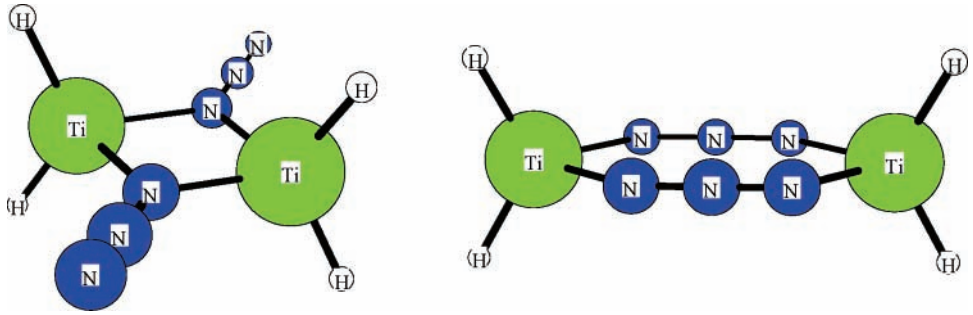

Figure 4. Three-dimensional plots of "end-on" $Ti_2(\mu\text{-}1,1\text{-}NNN)_2H_4$ and "linear" $Ti_2(\mu\text{-}1,3\text{-}NNN)_2H_4$ from a two-electron, two-orbital MCSCF/TZV(p) calculation.

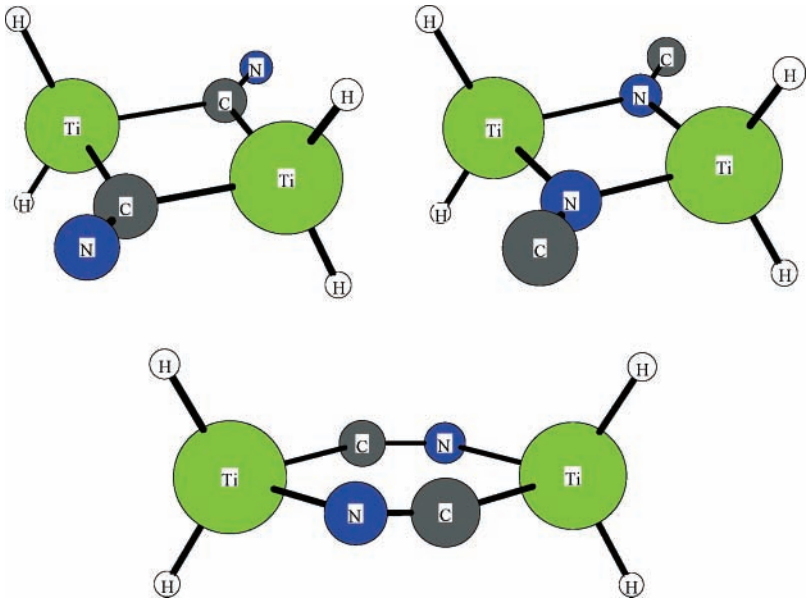

Figure 5. Three-dimensional plots of $Ti_2(\mu\text{-}1,1\text{-}CN)_2H_4$, $Ti_2(\mu\text{-}1,1\text{-}NC)_2H_4$, and $Ti_2(\mu\text{-}1,2\text{-}CN)_2H_4$ from a two-electron, two-orbital MCSCF/TZV-(p) calculation.

TABLE 6: Relative Energies (kcal/mol) for Lowest-Energy Singlet and Triplet States

	singlet			triplet		
compound	MRMP2/ TZV(p)	MRMP2/ TZVP(f)	MRMP2/ TZVP(fg)	MRMP2/ TZV(p)	MRMP2/ TZVP(f)	MRMP2/ TZVP(fg)
$H_2Ti(1,1\text{-}\mu\text{-}NNN)_2TiH_2$	0.0	0.0	0.0	3.0	3.2	3.2
$H_2Ti(1,3\text{-}\mu\text{-}NNN)_2TiH_2$	5.1	1.1	1.7	5.7	1.6	2.2
$H_2Ti(1,1\text{-}\mu\text{-}CN)_2TiH_2$	30.3	30.7	30.5	32.5	33.1	33.0
$H_2Ti(1,1\text{-}\mu\text{-}NC)_2TiH_2$	17.3	18.9	18.4	19.2	20.9	20.4
$H_2Ti(1,2\text{-}\mu\text{-}CN)_2TiH_2$	0.0	0.0	0.0	0.7	0.6	0.6
$H_2Ti(1,1\text{-}\mu\text{-}OCN)_2TiH_2$	26.3	49.5	49.4	26.8	50.0	49.9
$H_2Ti(1,1\text{-}\mu\text{-}NCO)_2TiH_2$	0.0	0.0	0.0	3.0	3.1	3.1
$H_2Ti(1,3\text{-}\mu\text{-}OCN)_2TiH_2$	1.9	9.3	9.6	2.0	9.3	9.7
$H_2Ti(1,1\text{-}\mu\text{-}ONC)_2TiH_2$	152.2	178.6	178.4	152.6	179.0	178.7
$H_2Ti(1,1\text{-}\mu\text{-}CNO)_2TiH_2$	170.7	176.6	177.0	173.7	179.9	180.3
$H_2Ti(1,1\text{-}\mu\text{-}ONC)_2TiH_2$	140.0	157.5	157.8	140.0	157.4	157.8
$H_2Ti(1,1\text{-}\mu\text{-}SCN)_2TiH_2$	47.4	46.7	47.1	47.5	46.8	47.2
$H_2Ti(1,1\text{-}\mu\text{-}NCS)_2TiH_2$	2.7	0.0	0.0	5.3	2.8	2.8
$H_2Ti(1,3\text{-}\mu\text{-}SCN)_2TiH_2$	0.0	0.7	1.1	0.0	0.7	1.1
$H_2Ti(1,1\text{-}\mu\text{-}NO)_2TiH_2$[a]	14.0	13.0	13.3	17.2	17.8	18.1
$H_2Ti(1,1\text{-}\mu\text{-}NO)_2TiH_2$[b]	56.8	55.0	57.3	57.1	55.3	57.6
$H_2Ti(1,1\text{-}\mu\text{-}ON)_2TiH_2$	96.8	111.5	113.6	97.0	111.8	113.8
$H_2Ti(1,2\text{-}\mu\text{-}NO)_2TiH_2$	0.1	0.2	0.2	0.0	0.0	0.0

[a] b_{2u} and b_{1g} frontier molecular orbitals. [b] a_g and b_{1u} frontier molecular orbitals.

is in the d_{xz} orbital, rather than $d_{x^2-z^2}$. This difference may be used to explain the dramatic difference in the magnetic coupling observed for the two bonding modes with the different metals. The HOMO and LUMO orbitals for titanium complexes are oriented along the Ti−Ti axis, whereas the orbitals in copper complexes are oriented along the Cu−ligand bonds.

CN. The cyano ligand can bridge the titanium atoms in three ways: two end-on structures (μ-1,1-CN and μ-1,1-NC) and one linear structure (μ-1,2-CN) (Figure 5). Experimentally, the cyano ligand has been observed to bind in a bidentate fashion using both the carbon and nitrogen or preferentially through the carbon when it bonds in an end-on fashion.[111] The end-on structure

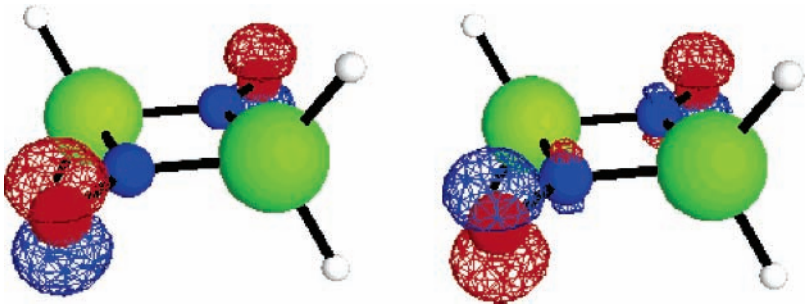

Figure 6. Three-dimensional plots of the natural orbitals for singlet $Ti_2(\mu\text{-}1,1\text{-}NO)_2H_4$ from a two-electron, two-orbital MCSCF/TZV(p) calculation. The orbital contour value for the plots is 0.1 bohr$^{3/2}$.

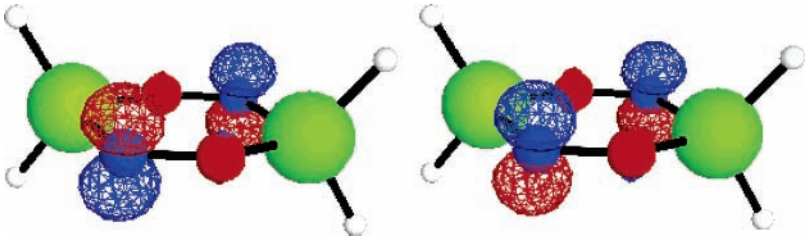

Figure 7. Three-dimensional plots of the frontier orbitals for triplet $Ti_2(\mu\text{-}1,2\text{-}NO)_2H_4$ from a ROHF/TZV(p) calculation. The orbital contour value for the plots is 0.1 bohr$^{3/2}$.

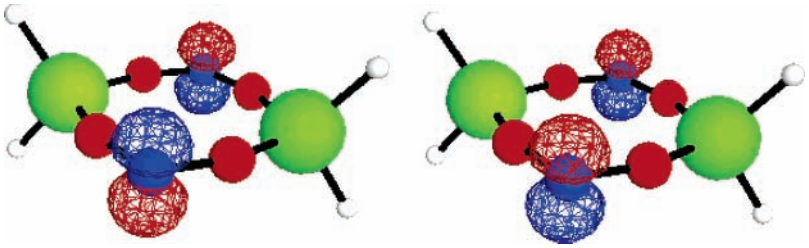

Figure 8. Three-dimensional plots of the natural orbitals from a two-electron, two-orbital MCSCF/TZV(p) calculation for singlet $Ti_2(NO_2)_2H_4$. The orbital contour value for the plots is 0.1 bohr$^{3/2}$.

TABLE 7: Isotropic Interaction Parameter *J* (cm^{-1})

molecule	bonding mode	MCSCF/ TZV(p)	MCSCF/ TZVP(f)	MCSCF/ TZVP(fg)	MRMP2/ TZV(p)	MRMP2/ TZVP(f)	MRMP2/ TZVP(fg)
$Ti_2(OH)_2H_4$	1,1-μ-O	−40	−43	−41	−118	−137	−135
$Ti_2(SH)_2H_4$	1,1-μ-S	−1	−47	−47	−32	−87	−87
$Ti_2(NH_2)_2H_4$	1,1-μ-N	−5	−5	−6	−8	−12	−12
$Ti_2(PH_2)_2H_4$	1,1-μ-P	−2	−6	−6	−34	−62	−62
$Ti_2(NNN)_2H_4$	1,1-μ	−183	−166	−164	−526	−566	−566
$Ti_2(NNN)_2H_4$	1,3-μ	−34	−13	−13	−103	−84	−86
$Ti_2(CN)_2H_4$	1,1-μ-C	−146	−133	−133	−391	−425	−430
$Ti_2(CN)_2H_4$	1,1-μ-N	−142	−99	−98	−337	−359	−362
$Ti_2(CN)_2H_4$	1,2-μ	−40	−21	−21	−115	−108	−110
$Ti_2(OCN)_2H_4$	1,1-μ-O	−29	−17	−17	−88	−84	−85
$Ti_2(OCN)_2H_4$	1,1-μ-N	−198	−162	−160	−518	−546	−547
$Ti_2(OCN)_2H_4$	1,3-μ	−6	−1	−1	−16	−10	−10
$Ti_2(ONC)_2H_4$	1,1-μ-O	−13	−14	−14	−55	−62	−63
$Ti_2(ONC)_2H_4$	1,1-μ-C	−163	−175	−175	−528	−575	−581
$Ti_2(ONC)_2H_4$	1,3-μ	2	2	2	5	5	5
$Ti_2(SCN)_2H_4$	1,1-μ-S	3	−4	−4	−6	−24	−24
$Ti_2(SCN)_2H_4$	1,1-μ-N	−155	−131	−130	−446	−490	−492
$Ti_2(SCN)_2H_4$	1,3-μ	−1	−3	−3	−4	−11	−11
$Ti_2(NO)_2H_4$	1,1-μ-N[a]	−158	−276	−276	−558	−831	−828
$Ti_2(NO)_2H_4$	1,1-μ-N[b]	−11	−10	−10	−49	−57	−57
$Ti_2(NO)_2H_4$	1,1-μ-O	−11	−7	−6	−35	−42	−42
$Ti_2(NO)_2H_4$	1,2-μ	8	24	24	26	34	35
$Ti_2(NO_2)_2H_4$	1,3-μ-ONO	4	5	5	−3	−6	−6

[a] b_{2u} and b_{1g} frontier molecular orbitals. [b] a_g and b_{1u} frontier molecular orbitals.

with D_{2h} symmetry is predicted to be a local minimum. For the linear structure, the highest possible symmetry is C_{2h}. (A structure with equally high C_{2v} symmetry could be imagined. However, since the two titanium atoms are in different environments, the C_{2v} structures were not considered in this study.)

For all three structures, the active orbitals are composed primarily of Ti $d_{x^2-z^2}$ orbitals, as discussed for the OH bridging ligand. Regardless of basis set, the MRMP2 calculations predict that the μ-1,2 arrangement is lower in energy than the μ-1,1-N structure by approximately 18 kcal/mol. The μ-1,1-C arrange-

TABLE 8: Comparison of Metal−Ligand−Metal Angle and Isotropic Interaction Parameters for D_{2h} Structures at the TCSCF/TZV(p) Level of Theory

	Ti−L−Ti angle	J (cm^{-1})
$Ti_2(1,1\text{-}\mu\text{-NCO})_2H_4$	96.4	−198
$Ti_2(1,1\text{-}\mu\text{-NNN})_2H_4$	99.6	−183
$Ti_2(1,1\text{-}\mu\text{-CNO})_2H_4$	92.3	−163
$Ti_2(1,1\text{-}\mu\text{-NO})_2H_4$[a]	99.1	−158
$Ti_2(1,1\text{-}\mu\text{-NCS})_2H_4$	96.9	−155
$Ti_2(1,1\text{-}\mu\text{-CN})_2H_4$	90.9	−146
$Ti_2(1,1\text{-}\mu\text{-NC})_2H_4$	96.7	−142
$Ti_2(\mu\text{-H})_2H_4$[b]	103.7	−98
$Ti_2(\mu\text{-OH})_2H_4$	102.4	−40
$Ti_2(1,1\text{-}\mu\text{-OCN})_2H_4$	104.2	−29
$Ti_2(1,1\text{-}\mu\text{-ONC})_2H_4$	107.8	−13
$Ti_2(1,1\text{-}\mu\text{-ON})_2H_4$	107.1	−11
$Ti_2(1,1\text{-}\mu\text{-NO})_2H_4$[c]	106.7	−11
$Ti_2(\mu\text{-Br})_2H_4$[d]	92.5	−4
$Ti_2(\mu\text{-Cl})_2H_4$[d]	95.7	7

[a] b_{2u} and b_{1g} frontier molecular orbitals. [b] Values from ref 29. [c] a_g and b_{1u} frontier molecular orbitals. [d] Values from ref 34.

ment is the highest energy bridging structure. These calculations suggest that the linear bonding structure will be preferred for the cyano ligand in this type of system.

OCN/ONC. The cyanato and fulminato ligands also have three available bridging modes. Experimentally, when it bonds in an end-on fashion the cyanato ligand tends to bind through the nitrogen atom[112] and the fulminato ligand tends to bind through the carbon atom.[111] For all of these structures, the usual D_{2h} or C_{2h} structure is a local minimum. The singlet states are essentially diradicals, with 0.85 to 1.00 electrons in the lowest virtual orbital (Table 2). For most of these compounds, the singlet state is the lowest in energy. However, the MRMP2 triplet state of $Ti_2(\mu\text{-}1,3\text{-ONC})_2H_4$ is predicted to be 0.03 kcal/mol lower in energy than the lowest energy singlet state (Table 3).

Larger basis sets and dynamic electron correlation also affect the isomeric orderings of these ligands. For the cyanato compounds at the MRMP2/TZV(p) level, $Ti_2(\mu\text{-}1,1\text{-NCO})_2H_4$ is 1.9 kcal/mol lower in energy than $Ti_2(\mu\text{-}1,3\text{-OCN})_2H_4$. The inclusion of higher polarization functions also stabilizes $Ti_2(\mu\text{-}1,1\text{-NCO})_2H_4$ with respect to $Ti_2(\mu\text{-}1,3\text{-OCN})_2H_4$. At the MRMP2/TZVP(fg) level, the relative energy is 9.6 kcal/mol. $Ti_2(\mu\text{-}1,1\text{-OCN})_2H_4$ is predicted to be much higher in energy than either of the other two compounds. For the fulminato compounds, at the MRMP2/TZV(p) level, the $Ti_2(\mu\text{-}1,3\text{-ONC})_2H_4$ compound is 12.2 kcal/mol lower in energy than the $Ti_2(\mu\text{-}1,1\text{-ONC})_2H_4$ compound. Multireference perturbation theory suggests that the μ-1,1-CNO and μ-1,1-ONC structures have similar energies. The calculations suggest that, for this system, the cyanato ligand will bind through the nitrogen atom

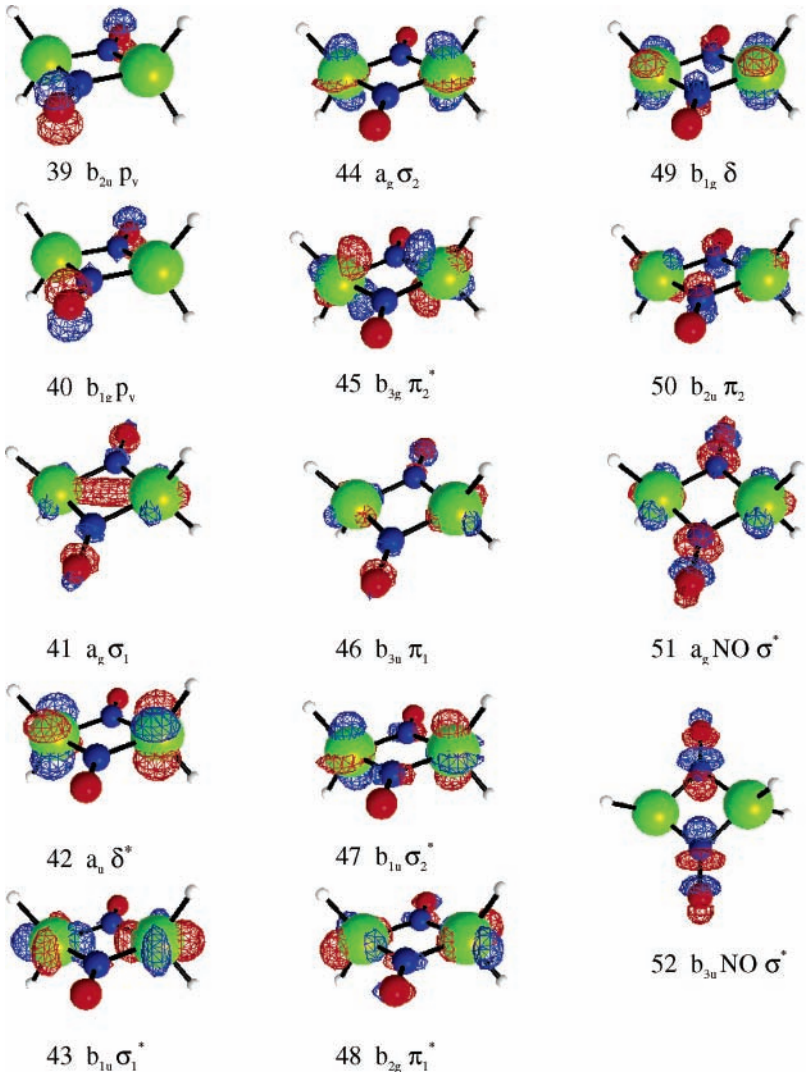

Figure 9. Three-dimensional plots of the 14 active molecular orbitals for $Ti_2(\mu\text{-}1,1\text{-NO})_2H_4$ used in the spin−orbit coupling calculations. Orbital 39 is the HOMO.

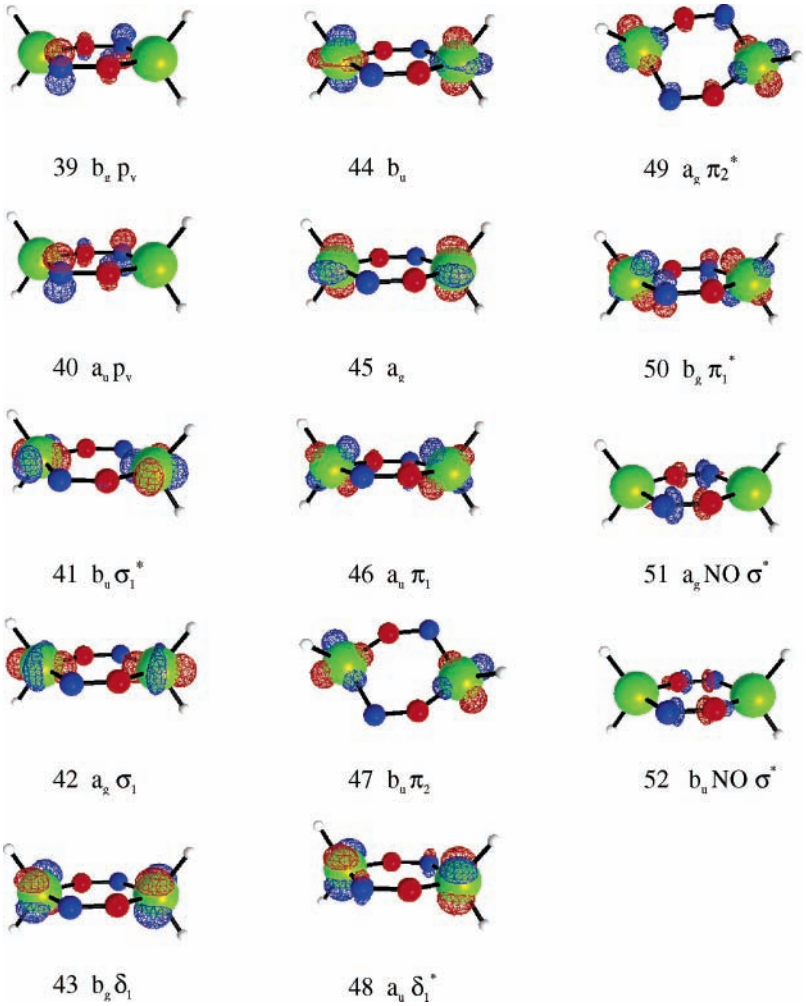

Figure 10. Three-dimensional plots of the 14 active molecular orbitals for $Ti_2(\mu\text{-}1,2\text{-}NO)_2H_4$ used in the spin−orbit coupling calculations. Orbital 39 is the HOMO.

in an end-on fashion and the fulminato ligand will bind in a linear fashion.

Many experimentally observed compounds with fulminato ligands are known to be explosive.[111] Indeed, the calculations on the compounds in this study show that the fulminato-bridged compounds are over 140 kcal/mol higher in energy than the cyanato-bridged compounds (Table 6), which suggests that the isomerization of these molecules would be highly exothermic.

SCN. The thiocyanate ligand also has three possible bridging modes. All three bridging structures have been observed experimentally in metal complexes.[113] The μ-1,3-SCN bridging structure has a C_{2h} local minimum. The bond angles for this compound are quite different from the bond angles for OCN (Table 5). The μ-1,1-N bridging mode has a local minimum with D_{2h} symmetry. However, the compound with the μ-1,1-S bridging mode in D_{2h} symmetry has one imaginary frequency for the singlet state and two for the triplet state. The lowest energy singlet with C_{2v} symmetry is 0.3 kcal/mol lower in energy than the related C_{2h} structure and 1.1 kcal/mol lower in energy than the D_{2h} structure (Table 6). The molecular orbitals in the active space are formed primarily from the Ti $d_{x^2-z^2}$ orbitals, as noted for the SH ligand. At the MRMP2/TZV(p) level, the singlet state is predicted to lie 0.03 kcal/mol below the triplet state (Table 3). As the basis set size is increased, the singlet is stabilized by a further 0.1 kcal/mol. At the MRMP2/TZVP(fg) level, the μ-1,1-NCS bridged structure is predicted to be 1.1 kcal/mol lower in energy. The μ-1,1-SCN bridged structure is predicted to be the highest in energy.

NO. Nitrosyl is an interesting ligand. Again, this ligand can bridge the titanium atoms in three possible ways. Two of these bridging modes (μ-1,1-NO and μ-1,2-NO) result in compounds with an electronic structure previously unseen in this study. The third bonding mode (μ-1,1-ON) has an electronic structure analogous to that described for the hydroxide complex.

The lowest energy singlet and triplet states for $Ti_2(\mu\text{-}1,1\text{-}NO)_2H_4$ are ^1A_g and $^3B_{3u}$. The frontier molecular orbitals that form these states have b_{2u} and b_{1g} symmetry and are shown in Figure 6. Rather than having unpaired electrons on the titanium atoms, this compound has the unpaired electron density mostly on the oxygen atoms. The two active molecular orbitals are principally formed from atomic p_y orbitals on the oxygen atoms. There are 0.87 electrons in the lowest virtual orbital, so the molecule is essentially a singlet diradical. At the MRMP2/TZV(p) level of theory, this ground-state singlet is 42.8 kcal/mol lower in energy than the first excited singlet state, which is composed of the normal titanium σ/σ^* orbitals (Table 6). MCSCF (2,14) calculations show that these states do not mix. The lowest energy triplet state is 2.8 kcal/mol higher in energy than the ground-state singlet at the MRMP2/TZV(p) level of theory. When the basis set size is increased, the state with the "normal" titanium σ/σ^* orbitals is predicted to lie approximately 40 kcal/mol higher in energy than the state created by the oxygen p_y orbitals. For $Ti_2(\mu\text{-}1,2\text{-}NO)_2H_4$, the lowest energy singlet and triplet states have ^1A_g and ^3B_u symmetry, respectively. The frontier molecular orbitals for these states have b_g and a_u symmetry and are shown in Figure 7. For this molecule, the

TABLE 9: First Four Spin States Obtained from the 20 Singlet, 20 Triplet SOC Calculation for $Ti_2(\mu\text{-}1,1\text{-}NO)_2H_4$[a]

spin state	principal axes	energy relative to adiabatic ground-state S_0 (cm^{-1})	CASSCF adiabatic state	eigenvector weighting
		CASSCF−SOC with HSO2 operator		
1		−12	S_0	0.9790
			T_2	0.0206
			T_9	0.0002
			T_7	0.0001
2	*X*	237	T_1	0.9951
			T_3	0.0045
			T_6	0.0002
			T_{10}	0.0002
3	*Y*	237	T_1	0.9952
			T_3	0.0045
			T_{10}	0.0002
			S_6	0.0001
4	*Z*	237	T_1	0.9956
			S_3	0.0039
			T_6	0.0002
			S_{11}	0.0002
		MCQDPT-SOC with HSO2 operator		
1		−2	S_8	0.5436
			S_0	0.4502
			S_{10}	0.0049
			S_2	0.0013
			T_7	0.0001
2	*Z*	9387	T_6	0.9996
			S_4	0.0002
			S_{15}	0.0001
3	*Y*	9387	T_6	0.9996
			T_5	0.0002
			T_{13}	0.0001
4	*X*	9388	T_6	0.9997
			T_5	0.0002
			T_{13}	0.0001

[a] Adiabatic state weightings are from the eigenvectors resulting from the diagonalization of the SOC matrix.

unpaired electron density is located primarily on the nitrogen atoms. The two active molecular orbitals are formed from the nitrogen p_z orbitals, where the *z*-axis is the principal axis. At the MRMP2/TZV(p) level of theory, the triplet is predicted to be 0.1 kcal/mol lower in energy than the singlet (Table 3).

Of the three bonding modes, the triplet state of $Ti_2(\mu\text{-}1,2\text{-}NO)_2H_4$ is predicted to be the lowest in energy. At the MRMP2/TZV(p) level, $Ti_2(\mu\text{-}1,1\text{-}NO)_2H_4$ and $Ti_2(\mu\text{-}1,1\text{-}ON)_2H_4$ are calculated to lie 14.0 and 96.8 kcal/mol above $Ti_2(\mu\text{-}1,2\text{-}NO)_2H_4$, respectively. With the larger basis set, the MRMP2 level of theory predicts that the $Ti_2(\mu\text{-}1,2\text{-}NO)_2H_4$ triplet structure will be lowest in energy. According to these calculations, the molecule is ferromagnetic and the magnetic susceptibility is predicted to increase as the temperature decreases. The effects of spin−orbit coupling on the singlet−triplet energy gap will be considered below.

NO_2. The nitrite ion is an electronegative ligand. While this ligand has many possible bonding modes (including μ-1,2-ONO and μ-1,3-ONO), the lowest energy local minimum found in this study is shown in Figure 8. The lowest energy singlet and triplet states are ^1A_g and $^3B_{3u}$, respectively. The frontier molecular orbitals are also shown in Figure 8. As seen in the μ-1,2-NO structure, the unpaired electron density is primarily located on the p_y orbitals of nitrogen, where the titanium atoms lie along the *z*-axis and the nitrogen atoms lie along the *x*-axis. The lowest energy singlet state has 0.99 electrons in the lowest virtual orbital, based on a natural orbital occupation analysis

TABLE 10: Principal Configuration State Functions in CASSCF Adiabatic States for $Ti_2(\mu\text{-}1,1\text{-}NO)_2H_4$[a]

state	coefficient	active orbital occupancy
S_0		
	0.172679	20000000000000
	−0.056019	+0000000000−00
	−0.439273	02000000000000
	0.509953	0+00000000−000
	0.640762	00020000000000
	−0.317496	00000000002000
S_8		
	−0.756819	20000000000000
	0.468181	+0000000000−00
	0.098792	02000000000000
	0.147722	0+00000000−000
	0.174700	00020000000000
	0.345678	00000020000000
	−0.098964	00000000002000
	−0.118790	00000000000200
T_1		
	0.749618	0+0+0000000000
	0.661282	000+000000+000
T_6		
	−0.692251	++000000000000
	0.449596	+000000000+000
	−0.253080	0+000000000+00
	0.464420	000+00+0000000
	0.197247	0000000000++00

[a] The occupancy of the 14 active orbitals in the primary CSFs is shown for four CASSCF adiabatic states. A "2" indicates that the orbital is doubly occupied in the CSF. A plus (+) or minus (−) indicates that a single electron occupies the orbital.

TABLE 11: First Four Spin States Obtained from the 20 Singlet, 20 Triplet SOC Calculation for $Ti_2(\mu\text{-}1,2\text{-}NO)_2H_4$[a]

spin state	principal axes	energy relative to adiabatic ground-state S_0 (cm^{-1})	CASSCF adiabatic state	eigenvector weighting
		CASSCF−SOC with HSO2 operator		
1		−2.870	S_0	0.9997
			T_2	0.0002
			T_6	0.0001
2	*Y*	887.082	T_1	0.9997
			T_3	0.0001
			T_7	0.0001
3	*X*	887.089	T_1	0.9997
			S_2	0.0001
			S_5	0.0001
4	*Z*	887.110	T_1	0.9997
			T_3	0.0002
			T_7	0.0001
		MCQDPT-SOC with HSO2 operator		
1		−0.730	S_0	0.5106
			S_{15}	0.3281
			S_7	0.1425
			S_{14}	0.0179
2	*X*	246.512	T_1	0.4628
			T_4	0.4238
			T_{20}	0.109
			T_5	0.0044
3	*Y*	246.630	T_1	0.4628
			T_4	0.4238
			T_{20}	0.109
			T_5	0.0044
4	*Z*	246.735	T_1	0.4628
			T_4	0.4238
			T_{20}	0.109
			T_5	0.0044

[a] Adiabatic state weightings are from the eigenvectors resulting from the diagonalization of the SOC matrix.

of the TCSCF/TZV(p) wave function (Table 2), so it is essentially a singlet diradical. The singlet−triplet splitting is

TABLE 12: Principal Configuration State Functions in CASSCF Adiabatic States for $Ti_2(\mu\text{-}1,2\text{-}NO)_2H_4$[a]

state	coefficient	active orbital occupancy	state	coefficient	active orbital occupancy
S_0			T_1		
	0.203232	20000000000000		−0.458774	++000000000000
	−0.313720	+000−000000000		0.102646	+000000+000000
	0.072045	+0000000000−00		−0.280084	+00000000+0000
	−0.530604	02000000000000		−0.636168	0+00+000000000
	0.147667	0+00000−000000		0.156088	0+000000000+00
	−0.496062	0+0000000-0000		−0.186759	0000+00+000000
	0.472163	00002000000000		0.474139	0000+0000+0000
	−0.115934	0000+000000−00		0.102556	000000000+0+00
	0.101962	0000000+0−0000	T_4		
	−0.239314	00000000020000		0.524968	++000000000000
S_7				−0.234767	+000000+000000
	−0.382972	20000000000000		0.207394	+00000000+0000
	0.318757	+000−000000000		−0.395514	0+00+000000000
	−0.308719	+0000000000−00		−0.302571	0+000000000+00
	−0.460314	0+00000−000000		0.067400	00++0000000000
	−0.238212	0+0000000-0000		0.364747	0000+00+000000
	0.352217	00002000000000		0.440483	0000+0000+0000
	0.298433	0000+000000−00		0.114145	0000000+000+00
	0.179306	00000002000000		−0.176248	000000000+0+00
	−0.309574	0000000+0−0000	T_5		
	−0.191792	00000000020000		−0.801000	00++0000000000
	−0.095493	00000000000200		0.306229	00+000+0000000
S_{14}				−0.067194	00+0000000+000
	0.076820	20000000000000		−0.068473	00+000000000+0
	0.060769	+000−000000000		0.376414	000+0+00000000
	0.059639	+0000000000−00		0.125356	000+0000+00000
	0.106808	00200000000000		0.223942	000+000000000+
	−0.618625	00+00000−00000		0.161946	00000++0000000
	0.113697	00+0000000000-		−0.092945	000000+000000+
	0.074314	000+00−0000000	T_{20}		
	0.593462	000+000000−000		−0.104177	++000000000000
	−0.088849	000+00000000−0		−0.739346	+000000+000000
	−0.280126	00000+00−00000		−0.197710	+00000000+0000
	−0.253416	000000+000−000		−0.231158	0000+00+000000
	−0.054223	00000002000000		−0.074468	0000+0000+0000
	−0.142897	00000000200000		0.573987	0000000+000+00
	−0.159228	00000000+0000-		0.113080	000000000+0+00
	0.080294	00000000002000			
S_{15}					
	0.508497	20000000000000			
	0.395347	+000−000000000			
	0.389969	+0000000000−00			
	−0.167991	02000000000000			
	−0.196134	0+00000−000000			
	0.054622	0+0000000-0000			
	0.091912	00+00000−00000			
	−0.092015	000+000000−000			
	0.304653	0000+000000−00			
	−0.362371	00000002000000			
	−0.295368	0000000+0−0000			
	0.165713	00000000000200			

[a] The occupancy of the 14 active orbitals in the primary CSFs is shown for eight CASSCF adiabatic states. A "2" indicates that the orbital is doubly occupied in the CSF. A plus (+) or minus (−) indicates that a single electron occupies the orbital.

0.03 kcal/mol at the MPMP2/TZVP(fg) level of theory (Table 3).

Magnetic Properties. A. Isotropic Interaction. The isotropic interaction between the titanium atoms in these dinuclear complexes is proportional to the calculated singlet−triplet energy gap, in the absence of spin−orbit coupling and magnetic dipole−magnetic dipole effects. The isotropic interaction parameters for these compounds are shown in Table 7. As noted earlier,[34] as the diradical character of the dinuclear complex becomes more pronounced and the natural orbital occupation numbers of the HOMO and LUMO approach 1, the ferromagneticity of the complex increases. At the MRMP2/TZVP(fg) level of theory, the interaction becomes more ferromagnetic (J becomes more positive) in the order $Ti_2(\mu\text{-}1,1\text{-}NO)_2H_4$ < $Ti_2(\mu\text{-}1,1\text{-}CNO)_2H_4$ < $Ti_2(\mu\text{-}1,1\text{-}NNN)_2H_4$ < $Ti_2(\mu\text{-}1,1\text{-}NCO)_2H_4$ < $Ti_2(\mu\text{-}1,1\text{-}NCS)_2H_4$ < $Ti_2(\mu\text{-}1,1\text{-}CN)_2H_4$ < $Ti_2(\mu\text{-}1,1\text{-}NC)_2H_4$ < $Ti_2(\mu\text{-}H)_2H_4$[29] < $Ti_2(\mu\text{-}Br)_2H_4$[34] < $Ti_2(\mu\text{-}OH)_2H_4$ < $Ti_2(\mu\text{-}1,2\text{-}CN)_2H_4$ < $Ti_2(\mu\text{-}SH)_2H_4$ < $Ti_2(\mu\text{-}1,3\text{-}NNN)_2H_4$ < $Ti_2(\mu\text{-}1,1\text{-}OCN)_2H_4$ < $Ti_2(\mu\text{-}1,1\text{-}ONC)_2H_4$ < $Ti_2(\mu\text{-}PH_2)_2H_4$ < $Ti_2(\mu\text{-}Cl)_2H_4$[34] < $Ti_2(\mu\text{-}1,1\text{-}ON)_2H_4$ < $Ti_2(\mu\text{-}1,1\text{-}SCN)_2H_4$ < $Ti_2(\mu\text{-}NH_2)_2H_4$ < $Ti_2(\mu\text{-}1,3\text{-}SCN)_2H_4$ < $Ti_2(\mu\text{-}1,3\text{-}OCN)_2H_4$ < $Ti_2(\mu\text{-}NO_2)_2H_4$ < $Ti_2(\mu\text{-}1,3\text{-}ONC)_2H_4$ < $Ti_2(\mu\text{-}1,2\text{-}NO)_2H_4$ < $Ti_2(\mu\text{-}F)_2H_4$.[34]

For copper compounds, an experimentally determined linear relationship was found between the isotropic interaction parameter J and the metal−ligand−metal angle.[114] However, the homodinuclear titanium compounds examined in this study show no such relationship (Table 8).

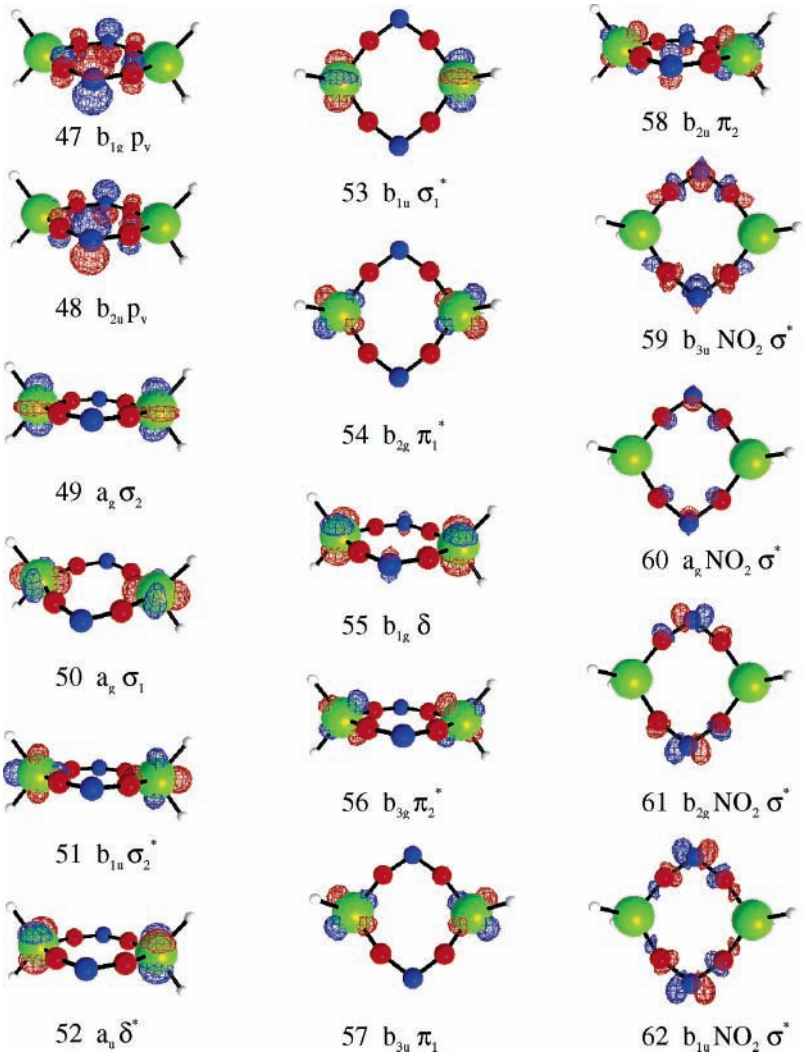

Figure 11. Three-dimensional plots of the 16 active molecular orbitals for $Ti_2(\mu\text{-}NO_2)_2H_4$ used in the spin−orbit coupling calculations. Orbital 47 is the HOMO.

B. Spin−Orbit Coupling Calculations. For the homodinuclear titanium molecules of interest in this study, it is necessary to consider 2 electrons in at least 10 orbitals in order to develop correct descriptions of the excited states.[30] The Ti−Ti bonding and antibonding interactions of the $\sigma\sigma^*$, $\pi\pi^*$, and $\delta\delta^*$ types arising from the atomic d orbitals must be treated. For all molecules except those with NO and NO_2 bridging ligands, an initial state-averaged 2-electron, 10-orbital MCSCF calculation was carried out at the ground-state geometry. For $Ti_2(\mu\text{-}1,3\text{-}ONC)_2H_4$, the ground state is predicted to be a triplet based on the TCSCF and MRMP2 calculations reported above, so the ROHF/TZV(p) geometry was used. For the other molecules, the calculations were performed at the TCSCF/TZV-(p) singlet geometry. The resulting orbitals were used in a second state-averaged 2-electron, 10-orbital MCSCF calculation with no orbital symmetry restraints and with each of the first 20 states weighted equally. These orbitals were used in both the CASSCF spin−orbit coupling (CASSCF−SOC) and MCQDPT spin−orbit coupling (MCQDPT-SOC) calculations. Earlier work on Ti_2H_6 examined the effects of systematically increasing the active space and the number of states included in the calculation and found that the above procedure was sufficient to capture the bulk of the spin−orbit coupling effects for these systems.[30]

For most of the homodinuclear titanium molecules considered in this study, the excited states and spin−orbit coupling effects are qualitatively similar to those previously reported for hydride and halide ligands.[30,34] However, the complexes with μ-1,1-NO, μ-1,2-NO, and μ-NO_2 ligands do not follow the customary trends. For the NO and NO_2 bridging ligands, more than 10 orbitals are needed to treat the low-lying excited states. To obtain starting orbitals, modified virtual orbitals were generated by removing six electrons in the usual manner.[115] For the μ-1,1-NO case, molecular orbitals formed primarily from atomic p orbitals on the oxygen atoms and antibonding molecular orbitals on NO were used in addition to the Ti d orbitals (see Figure 9). At the CASSCF−SOC level, the primary adiabatic states that mix to form the first spin state are S_0, T_2, T_9, and T_7 (see Table 9). T_1 is the primary component of spin states 2, 3, and 4. However, the inclusion of dynamic electron correlation dramatically alters these results. At the MCQDPT-SOC level, the first spin state is produced by a nearly equal mixture of S_8 and S_0. The principal adiabatic state that creates spin states 2, 3, and 4 is T_6. The primary configuration state functions (CSFs) (and their weightings) that contribute to these states are shown in Table 10. In Table 10, the occupancy of the 14 active orbitals (molecular orbitals 39−53, where orbital 39 is the HOMO) in each CSF is represented by an ordered pair of numbers. A 2 or

TABLE 13: First Four Spin States Obtained from the 20 Singlet, 20 Triplet SOC Calculation for $Ti_2(\mu\text{-}NO_2)_2H_4$[a]

spin state	principal axes	energy relative to adiabatic ground state S_0 (cm^{-1})	CASSCF adiabatic state	eigenvector weighting
		CASSCF-SOC with HSO2 operator		
1		−4.358	S_0	0.9995
			T_5	0.0004
			T_8	0.0001
2	*Y*	1281.284	T_1	0.9993
			T_6	0.0005
			T_3	0.0001
			T_7	0.0001
			S_7	0.0001
3	*X*	1281.292	T_1	0.9993
			T_6	0.0005
			T_3	0.0001
			T_9	0.0001
			S_{10}	0.0001
4	*Z*	1281.295	T_1	0.9993
			S_5	0.0005
			S_2	0.0001
			T_7	0.0001
			T_9	0.0001
		MCQDPT-SOC with HSO2 operator		
1		−2.862	S_0	0.9998
			T_5	0.0001
2	*Z*	1650.370	T_7	0.9998
			T_1	0.0001
			T_3	0.0001
3	*Y*	1650.378	T_7	0.9998
			S_2	0.0001
			T_1	0.0001
4	*X*	1651.108	T_7	0.9999
			T_3	0.0001

[a] Adiabatic state weightings are from the eigenvectors resulting from the diagonalization of the SOC matrix.

TABLE 14: Principal Configuration State Functions in CASSCF Adiabatic States for $Ti_2(\mu\text{-}NO_2)_2H_4$[a].

state	coefficient	active orbital occupancy
S_0		
	0.383051	2000000000000000
	−0.560557	+0000000−0000000
	−0.063039	0200000000000000
	−0.606029	0000020000000000
	0.409274	0000000020000000
T_1		
	0.654701	+0000+0000000000
	0.755765	00000+00+0000000
T_7		
	0.481309	++00000000000000
	−0.397813	+0000000000+0000
	0.404633	0+000000+0000000
	−0.541849	00000+000+000000
	0.390828	00000000+00+0000

[a] The occupancy of the 16 active orbitals in the primary CSFs is shown for three CASSCF adiabatic states. A "2" indicates that the orbital is doubly occupied in the CSF. A plus (+) or minus (−) indicates that a single electron occupies the orbital.

0 indicates that the orbital is doubly occupied or unoccupied, respectively. A plus (+) or minus (−) indicates that a single electron occupies the orbital. The antisymmetric spin function (for the singlet state) is donoted by a (+) and a (−), while the symmetric spin function (for the triplet state) is donoted by ++.

For $Ti_2(\mu\text{-}1,2\text{-}NO)_2H_4$, the ground state is predicted to be a triplet based on the TCSCF and MRMP2 calculations, so the ROHF/TZV(p) geometry was used. The 14 orbitals used in the SOC calculations are shown in Figure 10. The CASSCF-SOC calculations predict that the first spin state is primarily formed from the S_0 adiabatic state, while the next three spin states are primarily formed from the T_1 adiabatic state (see Table 11). At the MCQDPT-SOC level, the first spin state is composed of adiabatic states S_0, S_{15}, S_7, and S_{14}, while the next three spin states are composed of T_1, T_4, T_{20}, and T_5. The configuration state functions that create these states are shown in Table 12.

For $Ti_2(\mu\text{-}NO_2)_2H_4$, the ground state is predicted to be a triplet based on the TCSCF calculations, so the ROHF/TZV(p) geometry was used. The 16 orbitals used in the SOC calculations are shown in Figure 11. These include 10 orbitals primarily created from the Ti d atomic orbitals, two orbitals formed from N p orbitals, and four antibonding NO_2 orbitals. As shown in Table 13, the principal adiabatic states that form the first four spin states are S_0 and T_1 for CASSCF-SOC and S_0 and T_7 for MCQDPT-SOC. CSFs for these states are shown in Table 14.

The principal axes *X*, *Y*, and *Z* for the T_1 (lowest energy triplet state) components can then be determined from the coefficients of the eigenvectors. The axial and rhombic pseudodipolar parameters D_e and E_e can be calculated as discussed previously.[30] These values are presented in Table 15. In general, the one-electron operator (HSO1) and the partial two-electron operator (P2E) track the full two-electron operator (HSO2) closely. The magnitude of the state energies for the lowest singlet and triplet states calculated by HSO1 varies from HSO2 by up to 2.5 cm^{-1}, but details of the splittings are qualitatively correct. The energies calculated by P2E are practically the same as those of HSO2 and differ by no more than 0.021 cm^{-1}. In general, the magnitude of D_e and E_e increases as the spin−orbit coupling operator varies from HSO1 to P2E to HSO2. The magnitude of the zero-field splitting parameters from MCQDPT-SOC calculations is usually larger than the magnitude from CASSCF-SOC calculations. In general, the effect of dynamic correlation on the SOC parameters is much larger than is the effect of the SOC method.

4. Conclusions

The influence of multi-atom bridging ligands from groups 14, 15, and 16 of the periodic table on the magnetic properties of homodinuclear titanium complexes has been examined. These compounds are prototypes for many experimentally observed compounds. The compounds studied in this work have a high degree of diradical character, and there is little or no Ti−Ti bonding. Dynamic electron correlation is required for accurate predictions of the singlet−triplet splitting. In contrast to most of the ligands, NO^- and NO_2^- have the unpaired density on the ligands rather than the titanium atoms. The ferromagneticity of the complexes studied in this work is closely related to the natural orbital occupation numbers of the HOMO and LUMO but is not related to the titanium−ligand−titanium angle. The addition of dynamic correlation via second-order perturbation theory greatly increases the mixing of spin states, but there is very little singlet−triplet splitting.

The partial two-electron operator method tracks the full two-electron operator closely in the spin−orbit coupling calculations while dynamic correlation has a very large effect. The zero-field splitting parameters calculated by each operator method are very similar, although the magnitude tends to increase in the order HSO1 < P2E < HSO2. The zero-field splitting parameters from MCQDPT-SOC calculations are slightly larger than those from CASSCF-SOC calculations.

TABLE 15: Spin−Orbit Coupling

			CASSCF-SOC/TZV(p)			MCQDPT-SOC/TZV(p)		
			HSO1	P2E	HSO2	HSO1	P2E	HSO2
$Ti_2(OH)_2H_4$	1,1-μ-O	*S*	−12.563	−13.581	−13.584	−11.905	−13.413	−13.415
		T *X*	84.555	83.399	83.412	129.866	128.280	128.292
		T *Y*	84.507	83.345	83.355	129.847	128.279	128.288
		T *Z*	84.865	83.726	83.719	130.431	128.913	128.906
		D_e	0.334	0.354	0.335	0.575	0.634	0.616
		E_e	0.024	0.027	0.029	0.010	0.001	0.002
$Ti_2(SH)_2H_4$	1,1-μ-S	*S*	−10.554	−11.521	−11.522	−10.229	−11.515	−11.516
		T *X*	−4.436	−5.397	−5.400	8.088	6.832	6.829
		T *Y*	−4.475	−5.439	−5.437	8.030	6.759	6.761
		T *Z*	−4.439	−5.400	−5.396	8.085	6.848	6.851
		D_e	0.016	0.018	0.023	0.026	0.052	0.056
		E_e	0.019	0.021	0.019	0.029	0.036	0.034
$Ti_2(NH_2)_2H_4$	1,1-μ-N	*S*	−7.831	−8.486	−8.488	−7.454	−8.413	−8.414
		T *X*	6.814	6.132	6.138	22.425	21.408	21.414
		T *Y*	6.816	6.135	6.142	22.413	21.390	21.397
		T *Z*	6.932	6.259	6.256	22.539	21.558	21.555
		D_e	0.117	0.126	0.116	0.120	0.159	0.150
		E_e	−0.001	−0.002	−0.002	0.006	0.009	0.009
$Ti_2(PH_2)_2H_4$	1,1-μ-P	*S*	−11.862	−12.953	−12.954	−12.488	−14.118	−14.119
		T *X*	−3.208	−4.280	−4.284	10.070	8.497	8.494
		T *Y*	−3.264	−4.341	−4.339	9.969	8.373	8.376
		T *Z*	−3.221	−4.293	−4.289	10.006	8.424	8.428
		D_e	0.015	0.018	0.023	−0.013	−0.011	−0.007
		E_e	0.028	0.031	0.028	0.051	0.062	0.059
$Ti_2(NNN)_2H_4$	1,1-μ	*S*	−7.402	−8.058	−8.058	−7.225	−8.020	−8.021
		T *X*	461.455	460.679	460.684	828.690	827.341	827.347
		T *Y*	461.412	460.632	460.634	828.648	827.253	827.255
		T *Z*	461.549	460.779	460.775	829.038	827.682	827.677
		D_e	0.115	0.124	0.116	0.369	0.385	0.376
		E_e	0.022	0.023	0.025	0.021	0.044	0.046
$Ti_2(NNN)_2H_4$	1,3-μ	*S*	−11.649	−12.601	−12.601	−12.457	−13.903	−13.903
		T *X*	67.021	66.044	66.046	128.215	126.546	126.548
		T *Y*	66.993	66.013	66.014	128.122	126.450	126.451
		T *Z*	67.001	66.021	66.019	128.097	126.423	126.421
		D_e	−0.006	−0.008	−0.011	−0.072	−0.075	−0.078
		E_e	0.014	0.015	0.016	0.046	0.048	0.049
$Ti_2(CN)_2H_4$	1,1-μ-C	*S*	−12.995	−14.158	−14.159	−14.109	−15.881	−15.882
		T *X*	321.646	320.422	320.431	502.173	500.197	500.207
		T *Y*	321.476	320.237	320.240	501.995	500.034	500.040
		T *Z*	321.527	320.293	320.286	502.140	500.196	500.188
		D_e	−0.034	−0.037	−0.049	0.056	0.081	0.064
		E_e	0.085	0.093	0.095	0.089	0.082	0.083
$Ti_2(CN)_2H_4$	1,1-μ-N	*S*	−12.462	−13.579	−13.580	−13.642	−15.251	−15.253
		T *X*	328.904	327.584	327.595	520.840	518.461	518.476
		T *Y*	328.828	327.501	327.507	520.795	518.443	518.454
		T *Z*	329.055	327.746	327.739	521.706	519.452	519.444
		D_e	0.189	0.203	0.188	0.889	1.000	0.979
		E_e	0.038	0.042	0.044	0.023	0.009	0.011
$Ti_2(CN)_2H_4$	1,2-μ	*S*	−11.809	−12.825	−12.826	−12.167	−13.660	−13.660
		T *X*	75.418	74.358	74.359	117.219	115.218	115.220
		T *Y*	75.423	74.364	74.362	117.199	115.196	115.193
		T *Z*	75.439	74.381	74.384	118.485	116.650	116.653
		D_e	0.018	0.020	0.024	1.276	1.443	1.447
		E_e	−0.002	−0.003	−0.002	0.010	0.011	0.014
$Ti_2(OCN)_2H_4$	1,1-μ-O	*S*	−10.496	−11.416	−11.417	−10.834	−12.141	−12.143
		T *X*	55.346	54.387	54.395	131.234	129.821	129.829
		T *Y*	55.312	54.349	54.353	131.202	129.784	129.789
		T *Z*	55.372	54.413	54.408	131.319	129.914	129.908
		D_e	0.043	0.045	0.034	0.101	0.111	0.099
		E_e	0.017	0.019	0.021	0.016	0.019	0.020
$Ti_2(OCN)_2H_4$	1,1-μ-N	*S*	−9.734	−10.610	−10.611	−12.287	−13.814	−13.815
		T *X*	488.024	486.918	486.927	401.018	400.416	400.425
		T *Y*	487.965	486.853	486.858	398.687	397.956	397.960
		T *Z*	488.252	487.163	487.157	398.883	398.159	398.152
		D_e	0.258	0.278	0.264	−0.970	−1.027	−1.041
		E_e	0.030	0.032	0.035	1.165	1.230	1.233
$Ti_2(OCN)_2H_4$	1,3-μ	*S*	−13.701	−14.829	−14.829	−16.872	−18.807	−18.808
		T *X*	−1.015	−2.142	−2.140	4.975	2.471	2.473
		T *Y*	−1.004	−2.131	−2.132	5.164	3.211	3.209
		T *Z*	−1.005	−2.130	−2.129	7.156	5.350	5.354
		D_e	0.005	0.006	0.007	2.087	2.509	2.513
		E_e	−0.005	−0.006	−0.004	−0.095	−0.370	−0.368

TABLE 15 (Continued)

			CASSCF-SOC/TZV(p)			MCQDPT-SOC/TZV(p)		
			HSO1	P2E	HSO2	HSO1	P2E	HSO2
$Ti_2(ONC)_2H_4$	1,1-μ-O	*S*	−9.700	−10.545	−10.547	−9.542	−10.683	−10.684
		T *X*	17.453	16.586	16.593	70.534	69.318	69.325
		T *Y*	17.425	16.555	16.559	70.518	69.318	69.323
		T *Z*	17.459	16.592	16.587	70.563	69.368	69.364
		D_e	0.020	0.021	0.011	0.037	0.050	0.040
		E_e	0.014	0.015	0.017	0.008	0.000	0.001
$Ti_2(ONC)_2H_4$	1,1-μ-C	*S*	−11.744	−12.792	−12.792	−12.287	−13.814	−13.815
		T *X*	379.475	378.345	378.352	401.018	400.416	400.425
		T *Y*	379.338	378.195	378.198	398.687	397.956	397.960
		T *Z*	379.403	378.266	378.260	398.883	398.159	398.152
		D_e	−0.004	−0.004	−0.015	−0.970	−1.027	−1.041
		E_e	0.069	0.075	0.077	1.165	1.230	1.233
$Ti_2(ONC)_2H_4$	1,3-μ	*S*	−10.414	−11.322	−11.322	−11.883	−13.484	−13.484
		T *X*	−15.050	−15.955	−15.955	−17.540	−19.094	−19.094
		T *Y*	−15.042	−15.947	−15.948	−17.529	−19.107	−19.108
		T *Z*	−15.043	−15.948	−15.946	−17.539	−19.120	−19.118
		D_e	0.003	0.003	0.006	−0.005	−0.020	−0.017
		E_e	−0.004	−0.004	−0.003	−0.005	0.006	0.007
$Ti_2(SCN)_2H_4$	1,1-μ-S	*S*	−10.252	−11.198	−11.198	−10.260	−11.554	−11.554
		T *X*	−16.854	−17.796	−17.799	−1.767	−3.059	−3.062
		T *Y*	−16.875	−17.818	−17.817	−1.780	−3.076	−3.075
		T *Z*	−16.848	−17.789	−17.786	−1.748	−3.028	−3.024
		D_e	0.017	0.018	0.022	0.026	0.040	0.045
		E_e	0.011	0.011	0.009	0.007	0.008	0.007
$Ti_2(SCN)_2H_4$	1,1-μ-N	*S*	−10.913	−11.898	−11.900	−11.318	−12.619	−12.620
		T *X*	370.799	369.618	369.627	634.494	632.402	632.414
		T *Y*	370.738	369.552	369.557	634.483	632.371	632.379
		T *Z*	370.950	369.780	369.774	635.265	633.240	633.233
		D_e	0.182	0.195	0.182	0.776	0.853	0.836
		E_e	0.030	0.033	0.035	0.006	0.016	0.017
$Ti_2(SCN)_2H_4$	1,3-μ	*S*	−9.990	−10.885	−10.885	−9.973	−11.178	−11.178
		T *X*	−8.571	−9.466	−9.466	−1.810	−3.039	−3.039
		T *Y*	−8.562	−9.455	−9.456	−1.786	−3.013	−3.014
		T *Z*	−8.559	−9.452	−9.451	−1.658	−2.853	−2.852
		D_e	0.008	0.008	0.010	0.140	0.173	0.175
		E_e	−0.005	−0.005	−0.005	−0.012	−0.013	−0.013
$Ti_2(NO)_2H_4$	1,1-μ-N[a]	*S*	−10.529	−11.705	−11.710	−1.362	−2.193	−2.193
		T *X*	237.869	237.282	237.290	9388.05	9387.80	9387.80
		T *Y*	237.631	237.034	237.042	9387.54	9387.21	9387.20
		T *Z*	237.935	237.372	237.369	9387.38	9386.90	9386.90
		D_e	0.185	0.214	0.203	−0.419	−0.602	−0.599
		E_e	0.119	0.124	0.124	0.255	0.296	0.2965
$Ti_2(NO)_2H_4$	1,1-μ-N[b]	*S*	−13.67	−14.86	−14.86	−22.87	−25.79	−25.8
		T *X*	12.587	11.379	11.389	68.302	65.277	65.297
		T *Y*	12.556	11.344	11.352	68.268	65.23	65.248
		T *Z*	12.644	11.439	11.434	68.255	65.211	65.203
		D_e	0.0725	0.0775	0.0635	−0.03	−0.043	−0.069
		E_e	0.0155	0.0175	0.0185	0.017	0.0235	0.0245
$Ti_2(NO)_2H_4$	1,1-μ-O	*S*	−13.72	−14.87	−14.87	−15.75	−17.59	−17.59
		T *X*	7.204	6.012	6.024	54.265	52.184	52.199
		T *Y*	7.176	5.982	5.991	54.227	52.138	52.151
		T *Z*	7.268	6.08	6.074	54.418	52.347	52.34
		D_e	0.078	0.083	0.0665	0.172	0.186	0.165
		E_e	0.014	0.015	0.0165	0.019	0.023	0.024
$Ti_2(NO)_2H_4$	1,2-μ	*S*	−2.692	−2.87	−2.87	−0.684	−0.73	−0.73
		T *X*	887.27	887.09	887.09	246.63	246.51	246.51
		T *Y*	887.26	887.08	887.08	246.68	246.63	246.63
		T *Z*	887.29	887.11	887.11	246.83	246.74	246.74
		D_e	0.024	0.0235	0.0235	0.1755	0.1645	0.164
		E_e	0.003	0.0035	0.0035	−0.026	−0.059	−0.059
$Ti_2(NO_2)_2H_4$	1,3-μ-ONO	*S*	−4.102	−4.357	−4.358	−2.539	−2.861	−2.862
		T *X*	1281.6	1281.3	1281.3	1651.1	1651.1	1651.1
		T *Y*	1281.6	1281.3	1281.3	1650.5	1650.4	1650.4
		T *Z*	1281.6	1281.3	1281.3	1650.5	1650.4	1650.4
		D_e	0.008	0.01	0.007	−0.319	−0.372	−0.373
		E_e	0.005	0.004	0.004	0.318	0.365	0.365

[a] b_{2u} and b_{1g} frontier molecular orbitals. [b] a_g and b_{1u} frontier molecular orbitals.

Acknowledgment. This work was supported by a grant from the Air Force Office of Scientific Research. C.M.A. thanks the National Science Foundation for a Predoctoral Fellowship (2000−2003).

References and Notes

(1) Gatteschi, D.; Sessoli, R. *J. Magn. Magn. Mater.* **2004**, *272*−*276*, 1030.
(2) Coronado, E.; Forment-Aliaga, A.; Galán-Mascarós, J. R.; Giménez-Saiz, C.; Gómez-García, C. J.; Martinéz-Ferrero, E.; Nuez, A.; Romero, F. M. *Solid State Sci.* **2003**, *5*, 917.
(3) *Magnetism: Molecules to Materials IV*; Miller, J. S., Drillon, M., Eds.; WILEY-VCH: Weinheim, Germany, 2003.
(4) Miller, J. S.; Epstein, A. J. *MRS Bull.* **2000**, *25*, 21.
(5) *Metal-Organic and Organic Molecular Magnets*; Day, P., Underhill, A. E., Eds.; The Royal Society of Chemistry: Cambridge, U.K., 1999.
(6) *Molecular Magnetism: New Magnetic Materials*; Itoh, K., Kinoshita, M., Eds.; Gordon and Breach: Amsterdam, The Netherlands, 2000.
(7) Girerd, J.-J.; Journaux, Y. Molecular Magnetism in Bioinorganic Chemistry. In *Physical Methods in Bioinorganic Chemistry*; Que, L., Jr., Ed.; University Science Books: Sausalito, CA, 2000; p 321.
(8) Kahn, O. *Molecular Magnetism*; VCH: New York, 1993.
(9) Heisenberg, W. *Z. Physica* **1928**, *49*, 619.
(10) Boillot, M.-L.; Journaux, Y.; Bencini, A.; Gatteschi, D.; Kahn, O. *Inorg. Chem.* **1985**, *24*, 263.
(11) Kramers, H. A. *Physica* **1934**, *1*, 182.
(12) Anderson, P. W. *Phys. Rev.* **1950**, *79*, 350.
(13) Nesbet, R. K. *Ann. Phys.* **1958**, *4*, 87.
(14) Anderson, P. W. *Phys. Rev.* **1959**, *115*, 2.
(15) Nesbet, R. K. *Phys. Rev.* **1960**, *119*, 658.
(16) Wachters, A. J. H.; Nieuwpoort, W. C. Crystalfield Splitting and Magnetic Interaction in KNiF3. In *Selected Topics in Molecular Physics*; Clementi, E., Ed.; Verlag-Chemie: Weinheim, Germany, 1972; p 135.
(17) Bleaney, B.; Bowers, K. D. *Proc. R. Soc. London, Ser. A* **1952**, *214*, 451.
(18) Hay, P. J.; Thibeault, J. C.; Hoffmann, R. *J. Am. Chem. Soc.* **1975**, *97*, 4884.
(19) Kahn, O.; Briat, B. *J. Chem. Soc., Faraday Trans. 2* **1976**, *72*, 268.
(20) Kahn, O.; Briat, B. *J. Chem. Soc., Faraday Trans. 2* **1976**, *72*, 1441.
(21) de Loth, P.; Cassoux, P.; Daudey, J. P.; Malrieu, J. P., 1981.
(22) Illas, F.; Casanovas, J.; García-Bach, M. A.; Caballol, R.; Castell, O. *Phys. Rev. Lett.* **1993**, *71*, 3549.
(23) Pierloot, K.; Van Praet, E.; Vanquickenborne, L. G. *J. Phys. Chem.* **1993**, *97*, 12220.
(24) Casanovas, J.; Illas, F. *J. Chem. Phys.* **1994**, *100*, 8257.
(25) de Graaf, C.; Illas, F.; Broer, R.; Nieuwpoort, W. C. *J. Chem. Phys.* **1996**, *106*, 3287.
(26) Sousa, C.; de Jong, W. A.; Broer, R.; Nieuwpoort, W. C. *J. Chem. Phys.* **1997**, *106*, 7162.
(27) de Graaf, C.; Broer, R.; Nieuwpoort, W. C. *Chem. Phys. Lett.* **1997**, *271*, 372.
(28) Moedl, M.; Povill, A.; Rubio, J.; Illas, F. *J. Phys. Chem. A* **1997**, *101*, 1526.
(29) Webb, S. P.; Gordon, M. S. *J. Am. Chem. Soc.* **1998**, *120*, 3846.
(30) Webb, S. P.; Gordon, M. S. *J. Chem. Phys.* **1998**, *109*, 919.
(31) de Graaf, C.; de P. R. Moreira, I.; Illas, F.; Martin, R. L. *Phys. Rev. B* **1999**, *60*, 3457.
(32) Suaud, N.; Bolvin, H.; Daudey, J. P. *Inorg. Chem.* **1999**, *38*, 6089.
(33) de Graaf, C.; Sousa, C.; de P. R. Moreira, I.; Illas, F. *J. Phys. Chem. A* **2001**, *105*, 11371.
(34) Aikens, C. M.; Gordon, M. S. *J. Phys. Chem. A* **2003**, *107*, 104.
(35) Taratiel, D.; Cabrero, J.; de Graaf, C.; Caballol, R. *Polyhedron* **2003**, *22*, 2409.
(36) Herebian, D.; Wieghardt, K. E.; Neese, F. *J. Am. Chem. Soc.* **2003**, *125*, 10997.
(37) de Graaf, C.; Hozoi, L.; Broer, R. *J. Chem. Phys.* **2004**, *120*, 961.
(38) Wang, B.; Chen, Z. *Chem. Phys. Lett.* **2004**, *387*, 395.
(39) Muñoz, D.; de Graaf, C.; Illas, F. *J. Comput. Chem.* **2004**, *25*, 1234.
(40) Paulovic, J.; Cimpoesu, F.; Ferbinteanu, M.; Hirao, K. *J. Am. Chem. Soc.* **2004**, *126*, 3321.
(41) Illas, F.; de P. R. Moreira, I.; de Graaf, C.; Barone, V. *Theor. Chem. Acc.* **2000**, *104*, 265.
(42) Bodner, A.; Jeske, P.; Weyhermueller, T.; Wieghardt, K. E.; Dubler, E.; Schmalle, H.; Nuber, B. *Inorg. Chem.* **1992**, *31*, 3737.
(43) Jeske, P.; Wieghardt, K. E.; Nuber, B. *Inorg. Chem.* **1994**, *33*, 47.
(44) Lukens, W. W., Jr.; Andersen, R. A. *Inorg. Chem.* **1995**, *34*, 3440.
(45) Kempe, R.; Spannenberg, A.; Penlecke, N.; Rosenthal, U. *Z. Kristallogr.* **1998**, *213*, 423.
(46) Carr, S. G.; Boyd, P. D. W.; Smith, T. D. *J. Chem. Soc., Dalton Trans.* **1972**, 1491.
(47) Cookson, D. J.; Smith, T. D.; Pilbrow, J. R. *J. Chem. Soc., Dalton Trans.* **1974**, 1396.
(48) Fieselmann, B. F.; Hendrickson, D. N.; Stucky, G. D. *Inorg. Chem.* **1978**, *17*, 1841.
(49) Fieselmann, B. F.; Stucky, G. D. *Inorg. Chem.* **1978**, *17*, 2074.
(50) Fieselmann, B. F.; Hendrickson, D. N.; Stucky, G. D. *Inorg. Chem.* **1978**, *17*, 2078.
(51) Francesconi, L. C.; Corbin, D. R.; Hendrickson, D. N.; Stucky, G. D. *Inorg. Chem.* **1979**, *18*, 3074.
(52) Fachinetti, G.; Biran, C.; Floriani, C.; Villa, A. C.; Guastini, C. *J. Chem. Soc., Dalton Trans.* **1979**, *5*.
(53) Corbin, D. R.; Atwood, J. L.; Stucky, G. D. *Inorg. Chem.* **1986**, *25*, 98.
(54) Harris, H. A.; Rae, A. D.; Dahl, L. F. *J. Am. Chem. Soc.* **1987**, *109*, 4739.
(55) Harris, H. A.; Kanis, D. R.; Dahl, L. F. *J. Am. Chem. Soc.* **1991**, *113*, 8602.
(56) Rosenthal, U.; Goerls, H. *J. Organomet. Chem.* **1992**, *439*, C36.
(57) Cotton, F. A.; Dikarev, E. V.; Murillo, C. A.; Petrukhina, M. A. *Inorg. Chim. Acta* **2002**, *332*, 41.
(58) Briat, B.; Kahn, O.; Morgenstern-Badarau, I.; Rivoal, J. C. *Inorg. Chem.* **1981**, *20*, 4193.
(59) Chen, L.; Cotton, F. A.; Dunbar, K. R.; Feng, X.; Heintz, R. A.; Uzelmeir, C. *Inorg. Chem.* **1996**, *35*, 7358.
(60) Bercaw, J. E.; Brintzinger, H. H. *J. Am. Chem. Soc.* **1969**, *91*, 7301.
(61) Brintzinger, H. H.; Bercaw, J. E. *J. Am. Chem. Soc.* **1970**, *92*, 6182.
(62) Xin, S.; Harrod, J. F.; Samuel, E. *J. Am. Chem. Soc.* **1994**, *116*, 11562.
(63) Martin, R. L.; Winter, G. *J. Chem. Soc.* **1965**, 4709.
(64) Canty, A. J.; Coutts, R. S. P.; Wailes, P. C. *Aust. J. Chem.* **1968**, *21*, 807.
(65) Coutts, R. S. P.; Wailes, P. C.; Martin, R. L. *J. Organomet. Chem.* **1973**, *47*, 375.
(66) Jungst, R.; Sekutowski, D.; Davis, J.; Luly, M.; Stucky, G. *Inorg. Chem.* **1977**, *16*, 1645.
(67) Olthof, G. J. *J. Organomet. Chem.* **1977**, *128*, 367.
(68) Perevalova, E. G.; Urazowski, I. F.; Lemenovskii, D. A.; Slovokhotov, Y. L.; Struchkov, Y. T. *J. Organomet. Chem.* **1985**, *289*, 319.
(69) Hill, J. E.; Nash, J. M.; Fanwick, P. E.; Rothwell, I. P. *Polyhedron* **1990**, *9*, 1617.
(70) Sobota, P.; Ejfler, J.; Utko, J.; Lis, T. *J. Organomet. Chem.* **1991**, *410*, 149.
(71) Cotton, F. A.; Wojtczak, W. A. *Gazz. Chim. Ital.* **1993**, *123*, 499.
(72) Yu, P.; Murphy, E. F.; Roesky, H. W.; Lubini, P.; Schmidt, H.-G.; Noltemeyer, M. *Organometallics* **1997**, *16*, 313.
(73) Hao, S.; Feghali, K.; Gambarotta, S. *Inorg. Chem.* **1997**, *36*, 1745.
(74) Smith, S. B.; Stephan, D. W. In *Comprehensive Coordination Chemistry II*; McCleverty, J. A., Meyer, T. J., Eds.; Elsevier: Oxford, U.K., 2004; Vol. 4, p 31.
(75) Lappert, M. F.; Sanger, A. R. *J. Chem. Soc. A* **1971**, 874.
(76) Lappert, M. F.; Sanger, A. R. *J. Chem. Soc. A* **1971**, 1314.
(77) Armor, J. N. *Inorg. Chem.* **1978**, *17*, 203.
(78) Vroegop, C. T.; Teuben, J. H.; van Bolhuis, F.; van der Linden, J. G. M. *J. Chem. Soc. Chem. Commun.* **1983**, 550.
(79) Guggenberger, L. J.; Tebbe, F. N. *J. Am. Chem. Soc.* **1976**, *98*, 4137.
(80) Samuel, E.; Harrod, J. F.; Gourier, D.; Dromzee, Y.; Robert, F.; Jeannin, Y. *Inorg. Chem.* **1992**, *31*, 3252.
(81) Dick, D. G.; Stephan, D. W. *Can. J. Chem.* **1991**, *69*, 1146.
(82) Heneken, G.; Weiss, E. *Chem. Ber.* **1973**, *106*, 1747.
(83) Thewalt, U.; Schinnerling, P. *J. Organomet. Chem.* **1991**, *418*, 191.
(84) Fink, K.; Fink, R.; Staemmler, V. *Inorg. Chem.* **1994**, *33*, 6219.
(85) Kolczewski, C.; Fink, K.; Staemmler, V. *Int. J. Quantum Chem.* **2000**, *76*, 137.
(86) Ren, Q.; Chen, Z.; Ren, J.; Wei, H.; Feng, W.; Zhang, L. *J. Phys. Chem. A* **2002**, *106*, 6161.
(87) Wachters, A. J. H. *J. Chem. Phys.* **1970**, *52*, 1033.
(88) Hood, D. M.; Pitzer, R. M.; Schaefer, H. F., III. *J. Chem. Phys.* **1979**, *71*, 705.
(89) Rappe, A. K.; Smedley, T. A.; Goddard, W. A., III. *J. Phys. Chem.* **1981**, *85*, 2607.
(90) Dunning, T. H.; Hay, P. J. In *Methods of Electronic Structure Theory*; Schaefer, H. F., III, Ed.; Plenum Press: New York, 1977; p 1.
(91) Dunning, T. H. *J. Chem. Phys.* **1971**, *55*, 716.
(92) McLean, A. D.; Chandler, G. S. *J. Chem. Phys.* **1980**, *72*, 5639.
(93) Schmidt, M. W.; Baldridge, K. K.; Boatz, J. A.; Elbert, S. T.; Gordon, M. S.; Jensen, J. H.; Koseki, S.; Matsunaga, N.; Gordon, M. S.; Nguyen, K. A.; Su, S.; Windus, T. L.; Dupuis, M.; Montgomery, J. A., Jr. *J. Comput. Chem.* **1993**, *14*, 1347.

(94) Gordon, M. S.; Schmidt, M. W. *J. Mol. Struct. (THEOCHEM)*, in press.
(95) Webb, S. P.; Gordon, M. S. *J. Am. Chem. Soc.* **1995**, *117*, 7197.
(96) Glezakou, V.-A.; Gordon, M. S. *J. Phys. Chem. A* **1997**, *101*, 8714.
(97) Hirao, K. *Chem. Phys. Lett.* **1992**, *190*, 374.
(98) Hirao, K. *Chem. Phys. Lett.* **1992**, *196*, 397.
(99) Hirao, K. *Int. J. Quantum Chem.* **1992**, *S26*, 517.
(100) Hirao, K. *Chem. Phys. Lett.* **1993**, *201*, 59.
(101) Sunberg, K. R.; Ruedenberg, K. MCSCF Studies of Chemical Reactions: Natural Reaction Orbitals and Localized Reaction Orbitals. In *Quantum Science*; Calais, J.-L., Goscinski, O., Linderberg, J., Öhrn, Y., Eds.; Plenum: New York, 1976; p 505.
(102) Cheung, L. M.; Sunberg, K. R.; Ruedenberg, K. *J. Quantum Chem.* **1979**, *16*, 1103.
(103) Ruedenberg, K.; Schmidt, M. W.; Gilbert, M. M.; Elbert, S. T. *Chem. Phys.* **1982**, *71*, 41.
(104) Roos, B. O.; Taylor, P.; Siegbahn, P. E. M. *Chem. Phys.* **1980**, *48*, 157.
(105) Fedorov, D. G.; Finley, J. P. *Phys. Rev. A* **2001**, *64*, 042502.
(106) Koseki, S.; Gordon, M. S.; Schmidt, M. W.; Matsunaga, N. *J. Phys. Chem.* **1995**, *99*, 12764.
(107) Fedorov, D. G.; Gordon, M. S. *J. Chem. Phys.* **2000**, *112*, 5611.
(108) Bode, B. M.; Gordon, M. S. *J. Mol. Graphics Modell.* **1998**, *16*, 133.
(109) Comarmond, J.; Plumere, P.; Lehn, J. M.; Agnus, Y.; Louis, R.; Weiss, R.; Kahn, O. *J. Am. Chem. Soc.* **1982**, *104*, 6330.
(110) Sikorav, S.; Bkouche-Waksman, I.; Kahn, O. *Inorg. Chem.* **1984**, *23*, 490.
(111) Sharpe, A. G. In *Comprehensive Coordination Chemistry*; Wilkinson, G., Ed.; Pergamon Press: Oxford, U.K., 1987; Vol. 2, p 7.
(112) Schönherr, T. *Inorg. Chem.* **1986**, *25*, 171.
(113) Vrieze, K.; Van Koten, G. In *Comprehensive Coordination Chemistry*; Wilkinson, G., Ed.; Pergamon Press: Oxford, U.K., 1987; Vol. 2, p 189.
(114) Crawford, V. M.; Richardson, H. W.; Wasson, J. R.; Hodgson, D. J.; Hatfield, W. E. *Inorg. Chem.* **1976**, *15*, 3175.
(115) Bauschlicher, C. W. *J. Chem. Phys.* **1980**, *72*, 880.